

Detecting ratoon rice and mapping its distribution using machine learning algorithm and Sentinel-1 time-series data

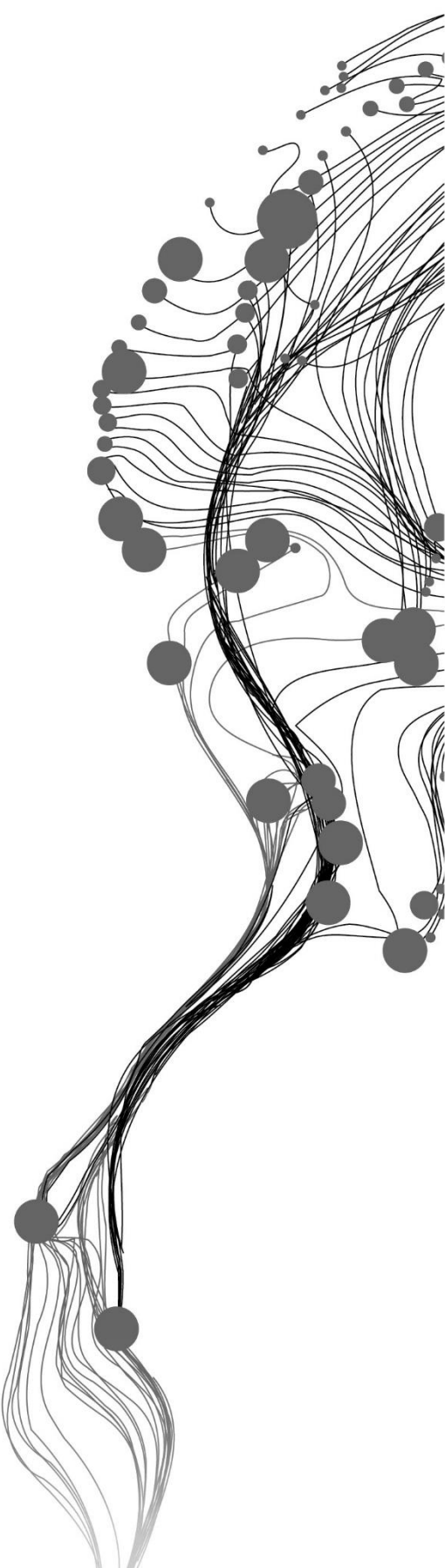
JITENDER RATHORE

June 2021

SUPERVISORS:

Dr. Roshanak Darvishzadeh

Prof. Dr. Andy Nelson



Detecting ratoon rice and mapping its distribution using a machine learning algorithm and Sentinel-1 time series data

JITENDER RATHORE

Enschede, The Netherlands, June 2021

Thesis submitted to the Faculty of Geo-Information Science and Earth Observation of the University of Twente in partial fulfilment of the requirements for the degree of Master of Science in Geo-information Science and Earth Observation.

Specialisation: [Natural resources management (NRM)]

SUPERVISORS:

Dr. Roshanak Darvishzadeh

Prof. Dr Andy Nelson

THESIS ASSESSMENT BOARD:

Dr T. Wang (Chair)

Dr A. Laborte (External Examiner, International Rice Research Institute)

DISCLAIMER

This document describes work undertaken as part of a programme of study at the Faculty of Geo-Information Science and Earth Observation of the University of Twente. All views and opinions expressed therein remain the sole responsibility of the author and do not necessarily represent those of the Faculty.

ABSTRACT

There is a large gap between rice production and consumption in the Philippines. Therefore, ratoon rice is practised to produce more rice on the same land with less labour and fertiliser; and without land preparations. Although mapping and detecting rice as the primary crop using remote sensing has received a deserved attention in the literature, mapping and detecting ratoon rice has been given less attention.

This study aims to detect ratoon and non-ratoon rice and its distribution using Sentinel-1 time series data and random forest algorithm in the Leyte, Iloilo, and Agusan del Sur provinces in the Philippines. Field data was provided by the International Rice Research Institute (IRRI) and included field survey data of a total of 317 fields, in which ratooning was practised in 47 fields. The pre-processed Sentinel-1 image data acquired during three growing seasons between 2017- 2019. Temporal backscatter behaviour of 60 rice fields in different polarisations and the Mann-Whitney U test were used to understand the differences between rice fields where ratooning was practised ($n=30$) and where it was not ($n=30$). Then, a random forest (RF) machine learning algorithm was used to discriminate between rice and ratoon rice. The predictive performance of the RF classification model was checked by overall accuracy and kappa values. The RF model was also performed to classify ratoon and non-ratoon rice crops using different ratoon growth stages. Finally, the distribution of ratoon and non-ratoon fields were mapped using a validated RF model.

In this study, we demonstrated that there is a clear difference in temporal backscatter of ratoon and non-ratoon rice crops. The results of the Mann-Whitney U test revealed that the backscatter of ratoon and non-ratoon fields when ratoon crops are at the flowering and ripening stages are significantly different in VH, VH/VV polarisations. When the random forest (RF) classifier was performed to discriminate ratoon, and non-ratoon classes, an overall accuracy (69.39%) and kappa value (0.39) were obtained. The RF model was calculated at different ratoon growing stages, demonstrated an overall accuracy of 44.44% at vegetative, 66.67% at flowering and 61.11% at ripening stages. The distribution of ratoon and non-ratoon rice fields showed that Iloilo province has the majority of fields with ratoon rice.

We concluded that the sentinel-1 time series could detect ratoon and non-ratoon rice at different stages using the RF model. The difference in ratoon and non-ratoon could be studied using VH polarisation and VH/VV ratio at the ripening stage where mean values of temporal backscatter were $\text{dB} > 1$. Also, the VH and VH/VV were statistically significant at the flowering stage. Hence more samples are required to study if ratoon and non-ratoon fields can be discriminated at this stage.

Further study in provinces where ratoon and non-ratoon are practised should also be explored.

Keywords: Sentinel-1 time series, ratoon and non-ratoon rice, random forest, Mann-Whitney U test

ACKNOWLEDGEMENTS

I want to thank many people who have contributed to the results in many ways:

To commence with, I would like to express my gratitude to the Faculty of Geo-Information Science and Earth Observation of the University of Twente for providing me UT-ITC excellence scholarship for studies at the Faculty of Geo-Information Science and Earth Observation of the University of Twente, Netherlands.

After, I express my sincere and deepest gratitude to my supervisor's Dr Roshanak Darvishzadeh and Prof. Dr Andy Nelson from the department of natural resources, ITC. I would also like to thank IRRI for providing the Sentinel-1 time series data for completing my study.

Dr Roshanak Darvishzadeh and Prof. Dr Andy Nelson encouraged me to make critical suggestions and pose challenging questions through numerous initial versions of my text. Their expertise, invaluable guidance, constant encouragement, and healthy criticism added considerably to my experience. Without their continual inspiration, it would not have been possible to complete this study.

I would like to thank Dr T. Wang as the Chairman of the thesis assessment board for the valuable suggestions and discussion.

I genuinely respect the contributions of all my colleagues. They provided selfless support, timely encouragement, thoughtful attitude, and ongoing help throughout the learning process.

I am deeply grateful to my parents and friends. They form part of my vision, teach me the essential and beautiful things in life, provide me with continuous encouragement, divine existence, and support me spiritually.

TABLE OF CONTENTS

1.	INTRODUCTION.....	1
1.1.	Background.....	1
1.2.	Research problem.....	5
1.3.	Research aim and objectives.....	6
1.3.1.	Specific Objectives:.....	6
1.4.	Research Questions.....	6
1.5.	Research Hypothesis.....	6
2.	MATERIALS AND METHODS	7
2.1.	Study area.....	7
2.2.	Field Data.....	8
2.3.	Sentinel -1 SAR.....	11
2.4.	Method	13
2.4.1.	Pre-processed data.....	14
2.4.2.	Temporal backscatter from VV and VH polarisations and statistical significance differences tests.....	14
2.4.3.	Random forest.....	14
2.4.4.	Accuracy assessment/validation.....	16
2.5.	Software	16
3.	RESULTS	17
3.1.	Temporal signature of ratoon and non-ratoon rice.....	17
3.2.	Selection of ratoon and non-ratoon dataset for significance test	19
3.2.1.	Sub-selection of ratoon dataset.....	19
3.2.2.	Selection of non-ratoon dataset.....	20
3.3.	Mean backscatter values in different growth stages using VV, VH and VH/VV polarisations	20
3.4.	Mann-Whitney U test: Significance test	23
3.5.	Classification: Random forest	24
3.5.1.	Confusion matrix: trained data model.....	24
3.5.2.	Variable importance of the trained model	25
3.5.3.	Confusion matrices: Prediction data.....	25
3.5.4.	Random forest classification with prediction dataset at different growing stages.....	26
3.6.	Distribution of ratoon and non-ratoon rice crop.....	28
4.	DISCUSSION.....	31
4.1.	Temporal backscattering behaviour of ratoon and non- ratoon rice in VV, VH and VH / VV polarisations.....	31
4.2.	RF-based classification	32
4.3.	Limitations	33
4.4.	Recommendations.....	34
5.	CONCLUSION.....	35
6.	LIST OF REFERENCES.....	37
7.	APPENDICES	42

LIST OF FIGURES

Figure 2.1: Study Area. Map shows the location of three provinces of Iloilo, Leyte, and Agusan del Sur in the Philippines.....	8
Figure 2.2: Study area and selected field samples	10
Figure 2.3: Methodology Flowchart.....	13
Figure 2.4: Random forest procedure modified based on Feng, Sui, Tu, Huang, & Sun (2018).....	15
Figure 3.1: Temporal signature of ratoon (pink) and non-ratoon (black dotted) rice crop in VH polarisation in the study region of Iloilo during wet season 2018.....	18
Figure 3.2: Temporal signature of ratoon (pink) and non-ratoon (black dotted) rice crop in VV polarisation in the study region of Iloilo during wet season 2018.....	18
Figure 3.3: Temporal signature of ratoon (pink) and non-ratoon (black dotted) rice crop in VH/VV ratio polarisation in the study region of Iloilo during wet season 2018.....	18
Figure 3.4: Box plot presenting the temporal backscatter variation in ratoon and- non-ratoon at different ratoon growth stages using VH (N= 60).....	22
Figure 3.5: Box plot presenting the temporal backscatter variation in ratoon and non-ratoon at different ratoon growth stages using VV (N= 60)	22
Figure 3.6: Box plot presenting the temporal backscatter variation in ratoon and non-ratoon at different ratoon growth stages using VH/VV (N= 60)	23
Figure 3.7: Map showing the distribution of ratoon and non- ratoon rice based on field observation and predicted classification of selected polygons from Leyte province	28
Figure 3.8: Map showing the distribution of ratoon and non- ratoon rice based on field observation and predicted classification of selected polygons from Iloilo province	29
Figure 3.9: Map showing ratoon and non- ratoon rice distribution based on field observation and predicted classification of selected polygons from Agusan del Sur province.....	30

LIST OF TABLES

Table 2.1: Example of field data provided by IRRI.....	9
Table 2.2: Selected provinces and their number of fields with ratoon crop.....	9
Table 2.3: Specification of Sentinel-1 SAR.....	11
Table 2.4: Sentinel-1 time-series images in the study area from 2017-2019.....	12
Table 2.5: Start and end of Sentinel-1 time-series images in the study area from 2017-2019.....	12
Table 2.6: Processing software.....	16
Table 3.1: Selection of growth stages of ratoon rice crop.....	19
Table 3.2: Examples of parameters that were used for the selecting of non-ratoon fields.....	20
Table 3.3: Mean backscatter values of selected samples in VV, VH and VH/VV polarisations for ratoon and non-ratoon rice crop.....	21
Table 3.4: P -values from a Mann- Whitney U test in ratoon and non-ratoon rice crops using VV, VH, and VH/VV polarisations when ratoon crops are at growing stages (N= 60).....	24
Table 3.5: Confusion matrix and OOB error rate of RF classifier for ratoon and non-ratoon classes using VV, VH and VH/VV polarisations (N= 60).....	25
Table 3.6: Variable importance of the trained model.....	25
Table 3.7: Confusion matrix and obtained classification accuracies of ratoon and non-ratoon rice crops using prediction/test data.....	26
Table 3.8: Confusion matrix and obtained classification accuracies for non-ratoon and ratoon rice crops at vegetative stage using prediction data.....	26
Table 3.9: Confusion matrix and obtained classification accuracies for non-ratoon and ratoon rice crops at flowering stage using prediction/test data.....	27
Table 3.10: Confusion matrix and obtained classification accuracies for non-ratoon and ratoon rice crops at ripening stage using prediction/test data.....	27

1. INTRODUCTION

1.1. Background

Rice belongs to the *Oryza* genus; *Oryza sativa* is one species of rice, the other being *Oryza glaberrima*, and it is the second-most produced staple food crop in the world (Wang et al., 2020). The annual average global production was 782.00 million tons in 2018 (FAOSTAT, 2020). It is the oldest cultivated crop on Earth. Although rice is used as food in the whole world, it is mainly produced in developing countries where about 95% of rice production comes from (Santos et al., 2003). The global demand for rice is on the rise as the world population continues to increase: it is expected that the world population will reach up to 8.79 billion by 2100 (Vollset et al., 2020). As food demand for people and animal feed may expect to increase by 3 billion tonnes by 2050 (Doering & Sorensen, 2018), it is essential to secure food stability for the increasing population. Food security remains a key challenge for farmers, distributors & suppliers, and nations (Chauhan et al., 2015; Fikriyah et al., 2019).

Rice production in Asia and Southeast Asia

According to Bandumula (2018), approximately 90% of rice is produced and consumed in Asia. Thus, rice production and consumption in Asia is important to Asian food security. China is a leading rice-producing country, followed by India, Indonesia, Bangladesh, Vietnam, Thailand, Myanmar, Philippines, Pakistan and Cambodia (FAOSTAT, 2020). The Philippines produces and consumes a variety of rice and still imports a large quantity of rice from Southeast Asian countries, especially Vietnam and Thailand, which are top exporters in the same region (Dawe, 2013). The Philippines imports rice because consumption is higher than production, and the gap between production and consumption is increasing (Tibao, 2009). Therefore, Filipino farmers practice ratoon rice –ratoon rice is the second rice crop, which has a shorter growing period than rice as the main crop. The ratoon rice is normally practised after harvesting the main rice crop in many country regions to increase rice production per unit area. Filipino farmers started to practice ratoon rice because the land is limited, consumption is higher than production, climate and weather are vulnerable, and traditional methods are insufficient to increase production (Benedict A. Exconde, 2016). The USA, China, and India also practice rice ratooning, but very few studies explain detecting ratoon rice from rice.

Ratooning Rice

The ratooning of rice allows to generate tillers from the main crop's stubble and raise production per unit area over a shorter growing period compared to a second rice crop (Oad et al., 2002). The ratoon rice crop has shorter and thinner stems as compared to the primary rice crop due to less availability of nutrients; most of the nutrients already transported to the panicle of the main crops, this limits the growth of buds (Wang

et al., 2020). It is also suited to mono-cropped systems and lowland areas. Lowland area is also called flooded rice area, and it is developed as rainfed and irrigated in lowland regions. This rice ecosystem requires maximum flooded fields (60-80%) during the cropping period (Santos et al., 2003).

According to Setiawan et al. (2014), ratoon rice is usually practised in regions where running water is continuously accessible after the harvest of the primary rice crop. Since water is an essential input for growing plants and producing better quality yields, ratooning rice requires 1300-1900 mm water after the land preparation till planting time and starts filling phase to spikelet filling. The ratoon rice may give the highest yield if the water is fully flooded and the cutting height is between 0-5 cm (Setiawan et al., 2014). Sometimes, it is recommended that water depth should be between 5 to 15 centimetres during the growing season (Santos et al., 2003).

Faruq et al. (2014) reported in their research that at least 8% grain yield per plant can be produced from ratoon rice crop. The ratoon rice crop can increase rice production by more than 51% after harvesting rice as the main crop on the same field (Krishnamurthy, 1989). According to Shamiul Islam et al. (2008), ratoon (rice) crops are affected by fertiliser management. Fertilisers would increase crop leaf area index (LAI) and numbers of panicles per unit area, the number of grains per panicles, grain weight and reduced grain barrenness. Low yield from ratoon rice is because of improper land cultivation, low soil quality, difficulty in controlling weeds (Negalur et al., 2017). Therefore, proper maintenance should be carried out for getting high-quality yields from ratooning crops, like controlling pests, using fertiliser and irrigation (Setiawan et al., 2014). Lodging and risk of plant diseases are higher in ratooning rice as compared to the main rice crop; as a result, the quality of grain may decrease (Chen et al., 2018). Nevertheless, ratoon rice saves seeds and labour and increases production (Faruq et al., 2014).

Ratooning crop mapping with optical remote sensing

In response to the growing demand for food, timely information on crop production is required for every single crop, including ratoon crops. Remote sensing techniques can be used for crop mapping, detection, and estimating crop production (Bégué et al., 2018). Both active and passive remote sensing can be used for crop mapping and detection (Karthikeyan et al., 2020). Some studies have suggested that ratooning crops (including rice) can be mapped and detected using remote sensing. For example, Misra et al. (2014) showed in their studies that combinations of multi-temporal LISS-3 and AWiFS remote sensing data could be used to detect sugarcane ratoon crops from other classes. They used fuzzy classification, possibilistic c-means (PCM), normalised difference vegetation index (NDVI), and spectral separability analysis to classify ratoon sugarcane crops accurately. NDVI was used to discriminate different multispectral responses of crops, and Euclidean distance based spectral separability analysis was performed to minimise the spectral noise from the crop response.

Furthermore, fuzzy classification was used for detecting ratoon sugarcane accurately from other crops. Liu et al. (2015) showed that ratoon rice could be detected using canopy reflectance measurements obtained from GreenSeeker optical sensor (NTech industries, Ukiah, California, USA) and crop fields measurement.

According to Singla et al. (2018) study, it was possible to discriminate ratoon sugarcane from sugarcane and other crops using temporal vegetation indices like NDVI and RVI of Landsat 8 OLI sensors and phenological changes such as plantation, tillering, and crop growth stages. Additionally, a recent study by Liu et al. (2020) on mapping ratoon rice using a time series of Sentinel-2 images in central China showed that the ripening stage of ratoon rice fields could be detected using the yellowness index. The yellowness index is calculated using blue, green, and red reflectance bands of Sentinel-2 data and can detect crops maturity stages. Therefore, phenology-based algorithms can be used to discriminate between ratoon rice and other rice crops. Enhanced vegetation index (EVI) was then used to detect the greenness of the second season crop and remove the misclassification affected by stubbles left in the ground.

Optical remote sensing is based on 'top of canopy reflectance', and cloudy weather limits the optical sensors. Optical sensors cannot detect vegetation (crops) or objects during rainy and cloudy conditions (Nelson et al., 2014). In contrast, radar remote sensing can operate in all light conditions, including day or night, and penetrate through haze, smoke and clouds (Alonso-González & Hajnsek, 2019). Radar sensors use short pulses of electromagnetic radiation (EMR) at long wavelengths, for instance, microwave or radio wave part of the electromagnetic spectrum. When EMR interacts with objects in its path, it will either transmitted, reflected or scattered by scatters such as rocks and vegetation (Joshi et al., 2016). The radar antenna receives information or signal of returning radiation or backscatter, namely the relative and intensity phases. The backscatter intensity is affected by the size, direction, height, and chemical composition. It helps to distinguish between different components of plants like leaves, stalks and fruits and cropping patterns like mono, mixing, and rotation crops (Baghdadi et al., 2009; Son et al., 2018). Radar remote sensing accounts for many factors such as crop growth stages, leaf-ground, double bounce, plant height, soil moisture, flooding frequency, and biomass development when used for crop mapping and monitoring (Inoue et al., 2014; Nelson et al., 2014). Hence, it is suitable for rice monitoring and forecasting its production (Sharifi & Hosseingholizadeh, 2020).

The literature review shows that the paddy rice mapping using radar remote sensing imagery originally started in the 1990s when ERS-1 launched (Aschbacher et al., 1995). ERS-1, ERS-2, PALSAR/ALOS, and RADARSAT satellites sensors have been used to estimate planted rice crop area and map different growing stages of rice (Panigrahy et al., 1999; Miyaoka et al., 2012). RADARSAT and ERS-1 multi-temporal data have provided better rice fields extraction than SPOT/HRV multispectral data (Suga et al., 2000). Lam-Dao et al. (2007) showed that Envisat ASAR data with dual-polarisation could be used for rice monitoring in complicated cropping systems.

Among existing satellites, Sentinel-1 has dual-polarisation and high temporal and spatial resolution; hence can be used for rice mapping (Ozden et al., 2016).

Rice crop mapping with Sentinel-1 SAR

With the advance of technology, the capabilities of SAR satellites are improving with high spatial-temporal resolution and dual polarimetry (Ishitsuka, 2018). Due to the high temporal coverage, Sentinel-1 has made possible to monitor rice crop more precisely over large areas than satellites like ERS-1&2, JERS-1SAR, RADARSAT-1&2, and ALOS/PALSAR (Ozden et al., 2016). In addition, it has made it possible to estimate different growing stages such as sowing, maturity, pre-harvest harvesting seasons of rice crops (Nelson et al., 2014). Studies have shown that the analysis of VV and VH polarisations of Sentinel-1 data for crop mapping does not provide the same results. As such, Raviz et al. (2016) used the rule-based rice detection method and Sentinel-1 time-series SAR data for mapping rice area in central Luzon, Philippines and found that the overall accuracy of rice maps was 80% using VV and 76% using VH polarisations.

Moreover, Sentinel-1 cross-polarized (VH) data has shown the capability to detect rice fields and phenological parameters. Nguyen & Wagner (2017) discriminated various rice growth stages using VH backscatter time-series Sentinel-1 data. According to Lasko et al. (2018). VH polarisation gave more accurate results in double and single rice mapping than VV polarisation. VV is more sensitive and affected by flooding water and plant canopy structure than VH polarisation (Son et al., 2018). Also, Yang et al. (2018) found in their study of field-based rice classification using multitemporal Sentinel-1 and Landsat 8 OLI data that VH backscatter is more sensitive to rice growth than VV polarisation backscatter response. In their study, C-band VH polarisation obtained 91.38% and VV 90.20% accuracy for rice and non-rice areas classification. However, the backscatter responses from VV, VH and VV/VH polarisation may vary in different stages of plant growth, such as land preparation, early growing period, tilting and harvesting (Fikriyah et al., 2019). Additionally, backscatter responses of C-band VV and VH polarisations are low during the flooding time; and it increases until the plant height reaches a certain stage of growth (rice crop) (Sharifi & Hosseingholizadeh, 2020). During the growing stage, backscatter interacts with surface water and plant stem; this interaction causes direct scattering and double-bounce effect; as a result, VH increases and VV decreases (Yuzugullu et al., 2017). When moisture decreases in the near-surface area of the ripening and harvest time, the backscatter of the rice crop is starting to drop in both VV and VH (Torbick et al., 2017). Therefore, it can realise that VV and VH polarisation backscatter responses vary at different crop conditions and growth stages.

Machine learning algorithms for remote sensing classification

The supervised, semi-supervised and unsupervised classification methods are frequently used in remote sensing studies for landcover classification, crops mapping and monitoring. Image classification methods can be object and pixel-based. Supervised classification includes maximum likelihood, minimum mean distance, k-nearest neighbours, while unsupervised classification use k-mean, ISODATA, self-organising map (SOM) and hierarchical clustering methods (Li et al., 2014). Machine learning algorithms such as artificial neural network (Kavzoglu & Mather, 2003), random forest (Breiman, 2001), support vector machine (Vapnik & Cortes, 1995), and decision tree (Brodley & Friedl, 1997) are gaining more attention in

remote sensing and are also widely used for crop mapping and landcover classification (Ayele et al., 2018; Saini & Ghosh, 2018; Han et al., 2019).

Among these methods, random forest (RF) is a powerful and flexible nonparametric supervised machine learning algorithm (Breiman, 2001; Aung & Min, 2017). The RF can handle high dimensional, noisy, and multisource data with no overfitting, and it has a powerful ability to deal with large datasets efficiently; and it has a high-level interaction with predictors.

Several studies have used the RF machine learning algorithm for rice mapping. For example, Cai et al. (2019) have adopted RF for deriving phenological parameters (start of season & end of the season, length of season) for rice crop mapping classification using Sentinel-1 time-series backscatter and Sentinel-2 NDVI data. Also, Bazzi et al. (2019) presented a classification of rice crops and other crops using RF and Sentinel-1 time-series data. A study by Singha et al. (2019) also showed that the RF algorithm could classify rice and non-rice crops using Google Earth Engine and Sentinel-1 time-series data. Further, Sun et al. (2019) compared mapping crops (wheat and maize) in the agricultural region of Yangzi River, China, using RF, artificial neural networks (ANN), and support vector machine (SVM) algorithms with multisource satellites like Sentinel-1, Sentinel-2 and Landsat-8 data. They found that RF outperformed other methods for crop mapping and obtained higher accuracy than ANN and SVM methods supervised methods. The RF can manage large datasets with great flexibility and powerfulness and can be used to determine the importance of variables or features during the classification (Sun et al., 2019). As demonstrated by the above literature, the RF algorithm has great capability for rice mapping with high accuracy. Nevertheless, its performance for detecting ratoon rice and its distribution has not been examined yet.

1.2. Research problem

Review of the literature reveals that remote sensing has been used to map and characterise main crops in many studies, while less attention has been given to detect or map ratoon crops, like rice and their distribution. Lack of knowledge about the distribution of ratoon rice causes uncertainty regarding the estimates of actual crop production and yield and the additional production or yield that comes from ratoon rice. Hence it is necessary to detect the areas of ratoon rice fields. Remote sensing data can be used to detect ratoon rice and map its distribution. Supervised machine learning algorithms such as random forest have gained popularity for mapping rice crop. However, its potential for detecting ratoon rice and its distribution using Sentinel-1 time series data needs further investigation.

Therefore, in this study, Sentinel-1, time-series data, and RF machine learning algorithm will be utilised to address this knowledge gap.

1.3. Research aim and objectives

This study aims to detect ratoon rice and map its distribution in Leyte, Iloilo and Agusan del Sur in the Philippines using Sentinel-1 time series data and RF machine learning algorithm.

1.3.1. Specific Objectives:

1. To understand the differences between the temporal rice backscatter behaviour in different polarisations where ratooning is practised and where it is not.
2. To discriminate between rice and ratoon rice using random forest (RF) machine learning algorithm and Sentinel-1 time-series data.
3. To map the distribution of ratoon rice in Leyte, Iloilo, and Agusan del Sur in the Philippines.

1.4. Research Questions

1. What is the difference between the temporal backscatter behaviour of rice (as the main crop) and ratoon rice in different polarisations?
2. How rice (as the main crop) and ratoon rice can be accurately discriminated using random forest (RF) algorithm and Sentinel-1 time-series data?

1.5. Research Hypothesis

H0: There is no significant difference in temporal backscatter behaviour of rice and ratoon rice in different polarisations.

H1: There is a significant difference in temporal backscatter behaviour of rice (as the main crop) ratoon rice in different polarisations.

H0: Ratoon rice cannot be accurately discriminated using random forest (RF) algorithm and Sentinel-1 time-series data.

H1: Ratoon rice can be accurately discriminated using random forest (RF) algorithm and Sentinel-1 time-series data.

2. MATERIALS AND METHODS

This chapter describes the study area, data and methods used in this study. First, the description of the study area, field survey data, and radar remote sensing data are presented. Next, the statistical data analysis of ratoon and non-ratoon samples are described. Finally, Random Forest classification, the procedures for classification of ratoon and non-ratoon fields and the accuracy assessment of this classification are described.

2.1. Study area

The Philippines is a southeast Asian county with a tropical climate and intense monsoons and covers 300,000 square km. It combines about 7641 islands, and it is classified broadly into three island groups of Luzon, Mindanao and Visayas. This study will focus on three provinces of Iloilo, Leyte, and Agusan del Sur (Figure 2.1). The Iloilo province is situated on Panay island, and the total area is 4663.42 square km with five districts. The major portion of the land area is occupied by agricultural land, which is 3447.44 square km (73.93%). The province's season has been classified into two; January to May is dry, and June to December wet, and higher rainfall is recorded in the wet season compared to the dry season. The average temperature is around 24-27 degrees Celsius. The soil of this province is very fertile, which is suitable for crops like rice.

The province of Leyte covers a total area of 6313.33 square km. Coronas. (1920) has classified the Philippines climate into four types based on its rainfall distribution. The province of Leyte has Type IV climate, i.e., rainfall has an equal distribution all over the year in this province. However, the dry season considered from November to April and wet from May to October. The province has a great extent of crop cultivation, such as rice.

The Agusan del Sur province is in the southern region of the Philippines and is one of its largest provinces. The Agusan del Sur is divided into 13 municipalities. It covers approximately 8966 square km, and forest and rivers cover a large portion of the province. Moreover, the climate of this province is categorised as Type II, which means that the province has only wet season and no dry season. Maximum precipitation in the Agusan del Sur province is recorded from December to January (Landicho et al., 2016).

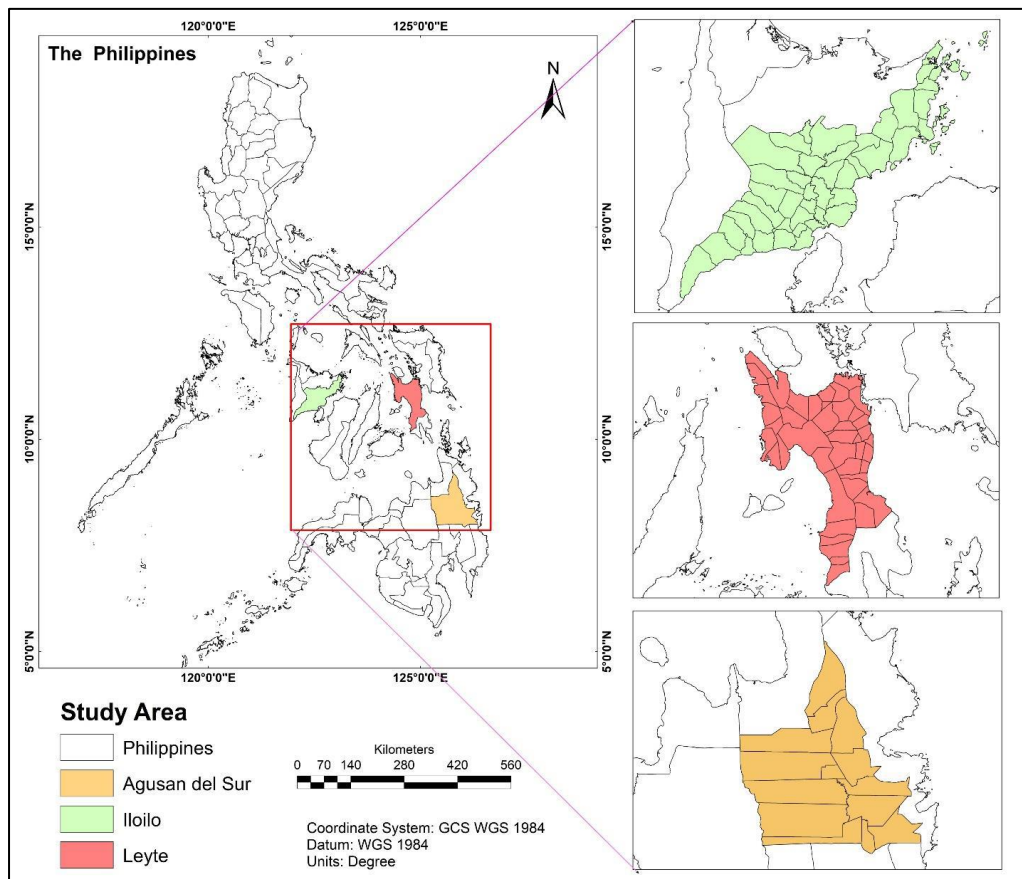


Figure 2.1: Study Area. Map shows the location of three provinces of Iloilo, Leyte, and Agusan del Sur in the Philippines

2.2. Field Data

The field data is provided by the International Rice Research Institute (IRRI) and was collected during the Pest Risk Identification and Management (PRIME) project between 2017 and 2019. The field survey data contain farmer interviews during three growing seasons between 2017 to 2019. The collected data cover 317 fields and include information about field geographical location, size, crop type, season, crop establishment date, harvesting date, irrigation system such as rainfed, irrigated and whether it is practised as ratoon field (Table 2.1).

DETECTING RATOON RICE AND MAPPING ITS DISTRIBUTION USING MACHINE LEARNING ALGORITHM AND SENTINEL-1 TIME SERIES DATA

In this study, ratoon and non-ratoon rice from Iloilo, Leyte, and Agusan del Sur provinces were extracted from the survey data collected during 2017- 2019. The number of field samples with ratoon rice in the three selected provinces was 42. To have an unbiased classification, a similar number of samples will be randomly selected from non-ratoon rice.

Table 2.1: Example of field data provided by IRRI

FID_crop_n	Brgy	Plot_size	Area_Qsqm	No_crops	Season	Crop	LandPDate	CropEDate	IrrigDate	AgFloodDate
F0101_0	Tangcarang	1,30	13.170		2 2019_dry	Rice	11_2_2018	11_4_2018	11_1_2018	11_1_2018
F0101_1	Tangcarang	1,30	13.170		2 2018_wet	Rice	7_1_2018	7_3_2018	6_4_2018	7_1_2018
F0102_0	Palamis	1,5	17.397		2 2019_dry	Rice	10_2_2018	11_1_2018	10_2_2018	10_4_2018
F0102_1	Palamis	1,5	17.397		2 2018_wet	Rice	5_3_2018	6_2_2018	5_2_2018	6_2_2018
F0103_0	Quibuar	1,2	11.161		3 2019_dry	Rice	12_3_2018	12_4_2018	12_3_2018	12_3_2018
F0103_1	Quibuar	1,2	11.161		3 2018_wet	Rice	9_2_2018	9_3_2018	9_1_2018	9_1_2018
F0103_2	Quibuar	1,2	11.161		3 2018_wet	Rice	5_4_2018	6_1_2018	5_4_2018	5_4_2018
F0104_0	Palamis	1,2	11.613		2 2019_dry	Maize		11_4_2018		
F0104_1	Palamis	1,2	11.613		2 2018_wet	Rice	5_4_2018	5_4_2018		
F0105_0	Macatiw	1,50	17.804		2 2019_dry	Rice	11_1_2018	11_2_2018	11_1_2018	11_4_2018
F0105_1	Macatiw	1,50	17.804		2 2018_wet	Rice	5_1_2018	5_3_2018	5_1_2018	5_3_2018
F0106_0	Amandiego	1,0	7.343		1 2019_dry	Fallow				
F0106_1	Amandiego	1,0	7.343		1 2018_wet	Rice	6_1_2018	6_3_2018		
F0107_0	Linmansangan	1,5	15.927		2 2019_dry	Fallow				
F0107_1	Linmansangan	1,5	15.927		2 2019_dry	Rice	9_1_2018	10_1_2018	9_1_2018	10_1_2018
F0107_2	Linmansangan	1,5	15.927		2 2018_wet	Rice	4_4_2018	5_4_2018	5_1_2018	5_3_2018
F0108_0	Tawintawin	0,6	6.022		1 2019_dry	Fallow				
F0108_1	Tawintawin	0,6	6.022		1 2018_wet	Rice	6_1_2018	6_4_2018		
F0109_0	Linmansangan	2,00	18.094		2 2019_dry	Rice	10_2_2018	11_1_2018	10_1_2018	11_2_2018
F0109_1	Linmansangan	2,00	18.094		2 2018_wet	Rice	6_2_2018	6_3_2018	6_1_2018	6_4_2018

The field data of rice crops have been provided by IRRI and included rice cropping information of 317 fields during three growing seasons from five provinces of the Philippines. Nevertheless, after exploring the provided dataset, it was revealed that there were only 47 fields in these provinces where ratoon rice has been practised as the second rice crop. In this research, the information of ratoon rice and rice as the main crop from Iloilo, Leyte, and Agusan del Sur- as main provinces where ratooning is practised studied (Figure 2.2). Table 2.2 shows the number of ratoon fields in these provinces. Hence, in total, 42 fields with ratoon crops from these three provinces were considered for further analysis. To have an unbiased classification, a similar number of samples will be randomly selected from non-ratoon rice.

Table 2.2: Selected provinces and their number of fields with ratoon crop

Region	Number of Ratoon Fields
Iloilo	12
Leyte	15
Agusan Del Sur	15
Total	42

Study area and selected field samples

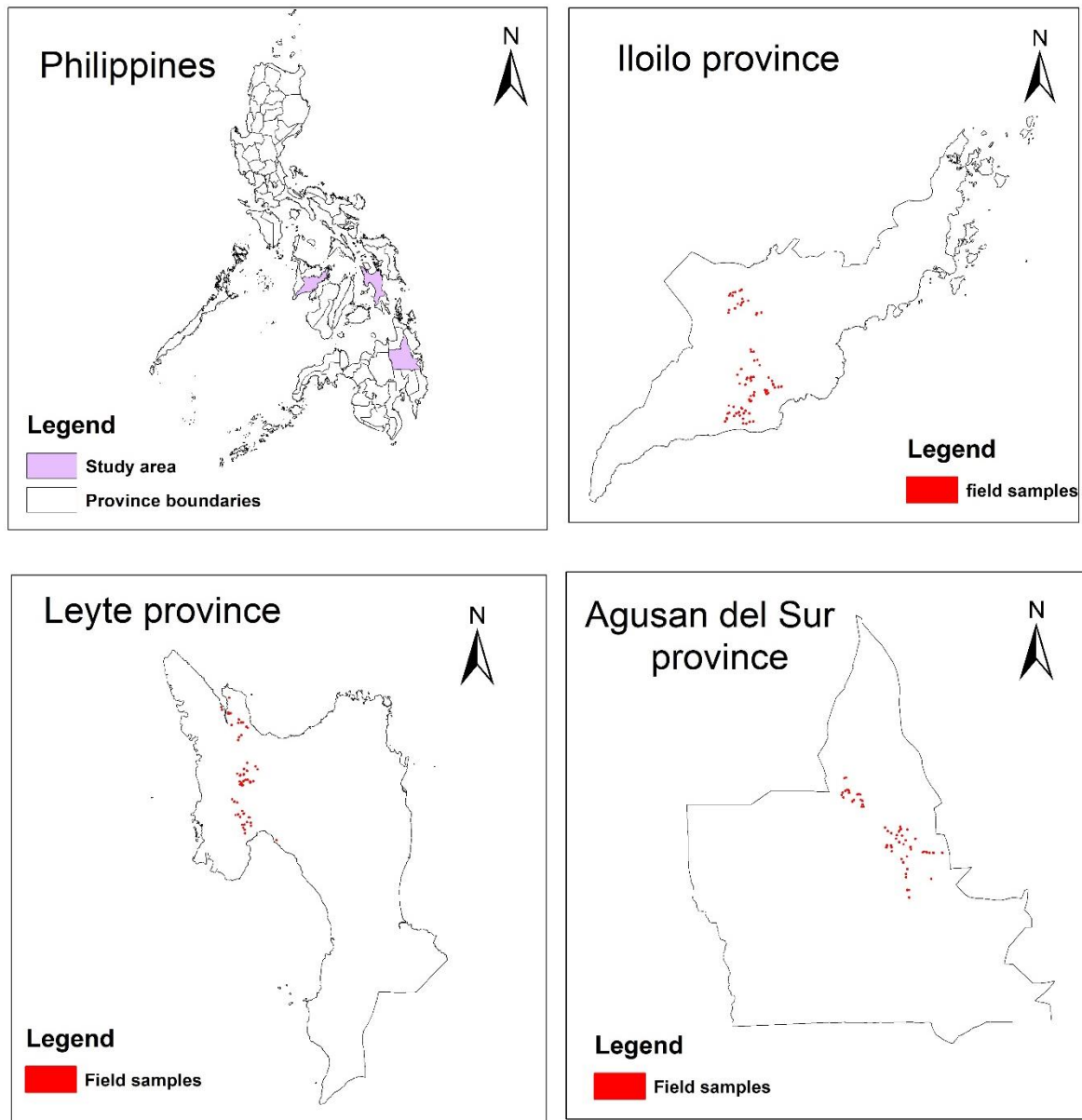


Figure 2.2: Study area and selected field samples

Figure 2.2 shows the distribution of surveyed rice fields within the study (in three provinces in the Philippines: Iloilo, Leyte and Agusan del Sur). The red points show the field samples of ratooned and non-ratooned rice crops

2.3. Sentinel -1 SAR

Sentinel-1 is a synthetic aperture radar satellite (SAR); it carries a C-band sensor with 5.405 GHz frequency and dual-polarisation, which means it contains both vertical (V) and horizontal (H), like VV+VH or VH+HH polarisations. The Sentinel-1A satellite was launched on 3 April 2014, and Sentinel-1B was launched on 22 April 2016. Sentinel-1 offers 3 days revisit times with ascending and descending passes at the equator (Geudtner et al., 2012). It provides a ground resolution of $5\text{m} \times 20\text{m}$ (Interferometric wide swath mode 250 km) and $20\text{m} \times 40\text{m}$ (Extra wide swath mode of 400 km) (Geudtner et al., 2014). Sentinel-1 has 175 days orbits/cycle for Sentinel-1A and Sentinel-1B satellites. It is located at 693 km altitude, and the inclination angle is 98.18 degrees. Sentinel-1 can collect data from all weather conditions, during the day or even at night or cloudy weather. The backscatter response by Sentinel-1 has been used for crop classification and discrimination from other crops. Table 2.3 provides detailed information about the Sentinel-1 (A& B) data.

Table 2.3: Specification of Sentinel-1 SAR

Parameters	Specification
Launch date	03 April 2014, S1-A 22 April 2016, S1-B
Inclination (angle)	98.18 degree
wave mode	20 km \times 20 km, 20 m \times 5 m resolution
Wavelength	5.405 GHz
Altitude	693 km
Orbit	Sun-synchronous near-polar
Polarization	VV+VH or HH+VH
Spatial Resolution	5 m \times 5 m
Repeat cycle	12 days
Interferometric Wide swath mode	240 km, 5 m \times 20 m resolution
Stripmap mode	80 km swath, 5 m \times 5 m resolution
Cycle length	175 days
Extra-wide swath mode	400 km swath

Table 2.4 shows the number of Sentinel-1 images taken for the study area in different seasons during 2017 – 2019, and Table 2.5 presents the time interval of sentinel -1 images acquisition for the three studied provinces. Acquisition of Sentinel-1 images for 2018 season-1 and 2019 season-1 starts September and ends in March, while for 2018 season-2, it starts in March and ends in September of the same year for all three selected provinces

Table 2.4: Sentinel-1 time-series images in the study area from 2017-2019

Provinces	2017-2019		
	2018 season-1	2018 season-2	2019 season-1
Iloilo	16	16	16
Leyte	16	17	16
Agusan del Sur	17	17	17

Table 2.5: Start and end of Sentinel-1 time-series images in the study area from 2017-2019

Provinces	2017-2019					
	Start	End	Start	End	Start	End
	2018 season-1		2018 season-2		2019 season-1	
Iloilo	9/16/2017	3/27/2018	3/27/2018	9/23/2018	9/11/2018	3/22/2019
Leyte	9/23/2017	3/22/2018	3/22/2018	9/30/2018	9/6/2018	3/29/2019
Agusan del Sur	9/18/2017	3/29/2018	3/29/2018	9/25/2018	9/13/2018	3/24/2019

2.4. Method

Figure 2.3 shows the methodological flow chart of the study. It presents the main steps such as pre-processing of Sentinel-1 data, extraction of average values, discrimination of ratoon and non-ratoon rice using temporal VV, VH and VV/VH ratio, and statistical analysis. Together with surveyed field data, the temporal backscatter responses used to train the RF algorithm and discriminate between ratoon and non-ratoon rice crops.

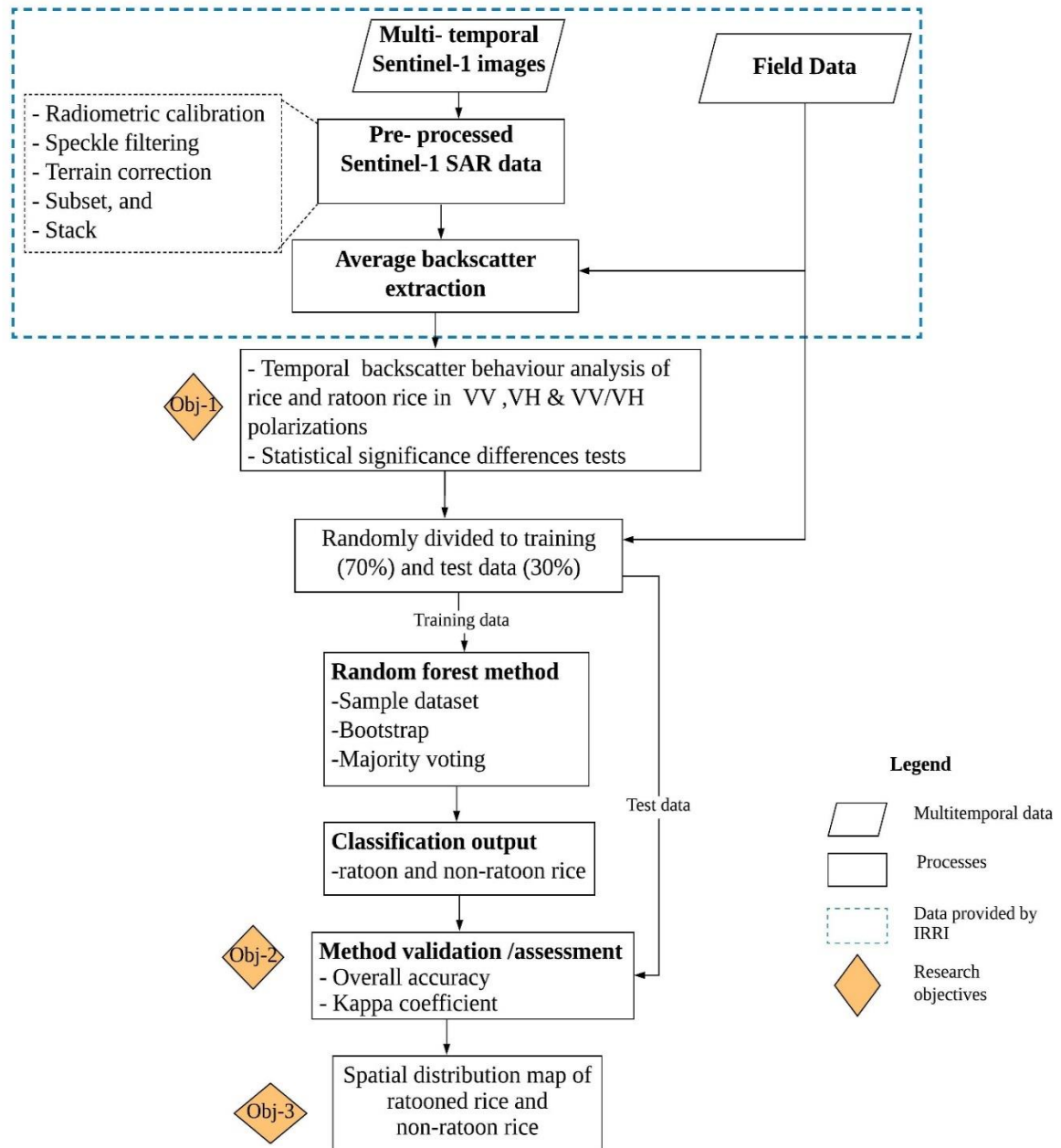


Figure 2.3: Methodology Flowchart

2.4.1. Pre-processed data

Pre-processing steps of Sentinel-1 data like removing speckling, radiometric calibration, subset, and stacking has already been done by IRRI. The average backscatter values of pixels falling within each field for VV, VH and VH/VV polarisations were later calculated by ITC as part of their contribution to the PRIME project.

2.4.2. Temporal backscatter from VV and VH polarisations and statistical significance differences tests

The temporal backscatter response of ratoon and non-ratoon fields from VV, VH & VH/VV polarisation were examined using the average backscatter values of each field. For this, the temporal backscatters of ratoon and no ratoon fields and their boxplots in VV, VH, and VH/VV ratio were plotted to understand the differences in backscatter behaviour between ratoon and ratoon non-ratoon fields.

For the statistical significance test, the Mann-Whitney U test conducted to assess whether there is a significant difference between temporal backscatter behaviour of ratoon rice and non-ratoon rice in VV, VH, and HV/VV polarisations. The Mann -Whitney U test is a nonparametric test that compares the difference between two independent groups or classes when samples are not normally distributed (Yap & Sim, 2011; Fikriyah et al., 2019). The analysis of temporal backscatter from different polarisations and significance tests were performed using SPSS software.

2.4.3. Random forest

Random forest (RF) is a nonparametric supervised machine learning algorithm (Breiman, 2001). RF is an improved version of tree classifiers, in which independent random vector sampling is used to generate classifiers from input vectors by casting a voting unit for popular classes (Breiman, 1999). RF has been used in remote sensing in various fields such as crop classification and mapping. It is easy to integrate multi-scale variables in RF; it has a powerful ability to deal with larger data sets efficiently and high-level interaction related predictors (Pal, 2005).

RF has been developed by creating a series of classification and tree- regressions (CARTs) (Torbick et al., 2017). The bootstrapping or resampling with replacement procedure applies to improve the varieties of classification trees, and it assigns every pixel to a class by following the highest voting number from a group of trees (Son et al., 2018). RF uses bootstrapping sampling (also called bagging in short) for random feature selection because bagging improves accuracy when random features are used. It can evaluate the strength of correlation and the generalisation error of the combined ensemble trees (Breiman, 2001). The RF uses the Gini index as an attribute selection metric, which estimates specific impurities related to classes (Breiman et al., 1984).RF classifies training samples data into two equal weights, and it uses randomisation processes to classify data. Randomisation processes include the random selection of a subset of training samples data for each tree and the selection of subset variables at every node of the trees (Im et al., 2016). Performance of the RF model can be checked by applying an internal cross-validation approach and using 70% samples data as used in bag samples for training tree, and 30 % samples data as out of the bag samples (Belgiu & Drăgu, 2016).

Figure 2.4 demonstrates the random-forest procedures for classifying the data into ratoon and non-ratoon classes. Sentinel-1 data and the field samples of ratoon and non-ratoon fields were split into training and test samples in the R open-source programming language. For data splitting, a proportion of 70% was considered as training samples and 30% as for the test samples. The bootstrapping technique was applied to the training samples. The bootstrapping creates a training sample with N- decision trees, and each tree predicts the output class as shown in the red circle. A majority voting selects the final classes.

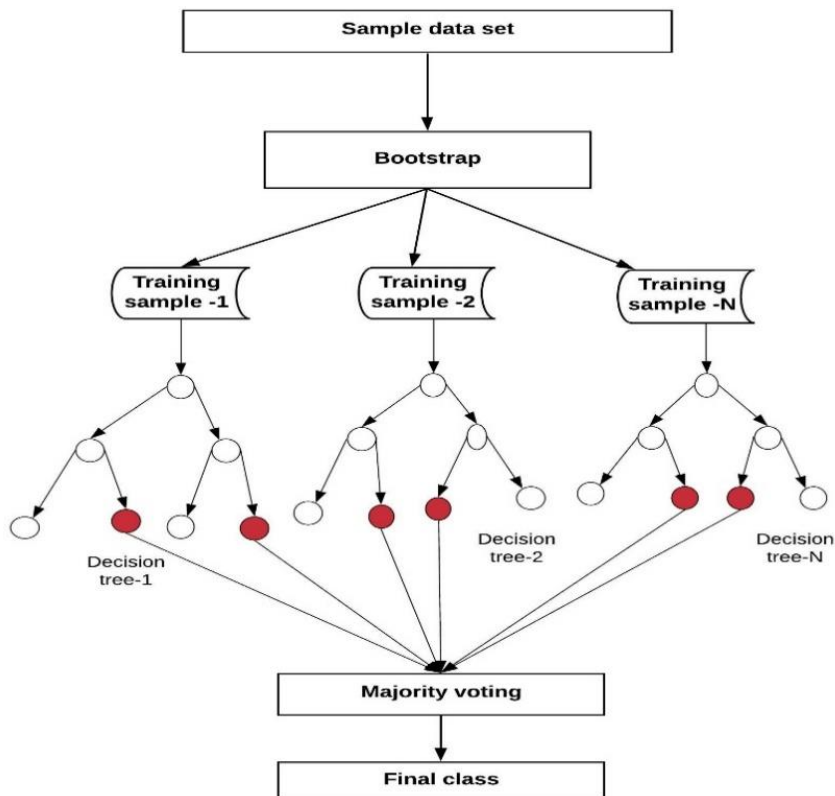


Figure 2.4: Random forest procedure modified based on Feng, Sui, Tu, Huang, & Sun (2018)

The confusion matrix describes the model's overall accuracy and kappa values. The producer and user accuracy can also calculate by a confusion matrix. The correctly classified classes determine the overall accuracy. Story & Congalton (1986) stated that producer and user accuracy evaluate the correctly classified individually category from samples. Kappa values all the time stay below or equal to 1. The kappa values below 0 show that the classifier model is useless for predicted classes, but the value is close to 1 indicate model fitness. Landis and Koch (1977) provided the scheme for interpreting the kappa values, such as the values between 0 to 0.2 with no agreement with the model and sample data. In addition, the fairness of the model determines values from 0.21 to 0.40, 0.41–0.60 (modest), 0.61–0.80 (considerable), and 0.81–1, roughly perfect with the model and sample data.

The Out-of-bag error (OBB) is an error evaluation method, which is usually practised to estimate the precision of random forest and decide suitable values for appropriate parameters. For instance, the number

of class predictors randomly selected for splitting is called mtry (Janitza & Hornung, 2018). The training dataset provided the OOB errors rates, which explained the model fitness. The higher OOB error rates mean the model is not applicable, while the lower OOB describes the model’s usefulness.

2.4.4. Accuracy assessment/validation

Bootstrapping in random forests protects against overfitting. The out-of-bag error estimates can be obtained using the mean prediction error of the trees that did not use training samples in their bootstrap. Therefore, validation to assess an unbiased evaluation of the results (as is the case for many other methods) may not be necessary. However, in this study, the cross-validation performed in the RF model using the training data, validation and the accuracy assessment were performed using randomly selected test (30%) data. The confusion matrix described the performance of the classifier model and showed the correctly classified features and overall accuracy. The accuracy measurement indicators such as overall accuracy and kappa value were selected for checking the RF algorithm’s performance. The R software applied to perform random forest classification and for accuracy assessment.

The validated RF model was used to map ratoon and non-ratoon samples in the study area of Iloilo, Leyte and Agusan del Sur. The predicted classified data divided into ratoon and non-ratoon rice crops. The comparison between field observations and predicted data also shown. The correctly classified ratoon and non-ratoon can easily compare through maps (See: appendix VIII, Sentinel-1 images used for validation RF model).

2.5. Software

Table 2.6 shows the software to be employed for analysis of Sentinel-1 time series and field data to discriminate between ratoon rice and rice as the main crop.

Table 2.6: Processing software

Name of software	Functions
Microsoft excel	<ul style="list-style-type: none"> • Field data analysis
Microsoft words	<ul style="list-style-type: none"> • MSC thesis writing, and • Other documentations
MATLAB/R/SPSS	<ul style="list-style-type: none"> • Analysis of sentinel-1 data, • Statistical tests to understand VV and VH temporal backscatter behaviour, and • R for RF classification
ArcGIS	<ul style="list-style-type: none"> • Map production

3. RESULTS

This chapter has five subsections. First, the temporal backscatter signature of ratoon and rice as a primary crop (non-ratoon rice) are studied. Then the sub-selection of ratoon samples and non-ratoon data selection has been presented. Further, backscatter values of ratoon and non-ratoon samples in different growth stages using VV, VH and VH/VV polarisations followed by the results of the Mann-Whitney U test are presented. Finally, the random forest classification results of ratoon and non-ratoon samples and their distribution in the study area are presented.

3.1. Temporal signature of ratoon and non-ratoon rice

It was essential to understand the temporal signature behaviour of ratoon as a second rice crop and non-ratoon as a primary rice crop in different seasons and different study sites. As such temporal signatures of ratoon and non-ratoon samples have been used to examine the variation of backscatter from different polarisations such as VV, VH and VH/VV at different growing seasons. The temporal signature can use to study crop different growth stages like vegetative, flowering, ripening, and harvesting. To understand the difference between ratoon and non-ratoon temporal signatures, their signatures were mainly studied after harvesting the primary rice when the ratoon crop started. Two fields with ratoon (ID 650) and non-ratoon rice (ID 661) have been selected for graphical representation and comparison. Land crop establishment (26 July 2018), crop ecosystem (rainfed), and harvesting dates are similar in both fields. Figure 4.1 shows the temporal signature of these two fields during wet season 2018 in Iloilo region using VV, VH and VH/VV polarisations. The temporal signatures allow understanding how the backscatter responses vary before and after harvesting ratoon and non-ratoon (primary) rice crops.

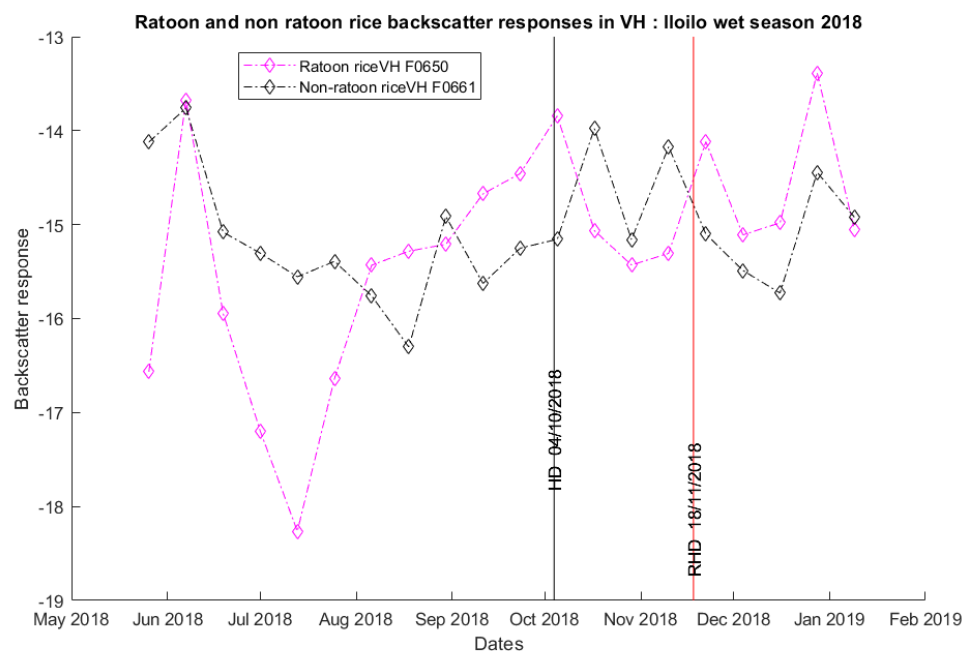


Figure 3.1: Temporal signature of ratoon (pink) and non-ratoon (black dotted) rice crop in VH polarisation in the study region of Iloilo during wet season 2018

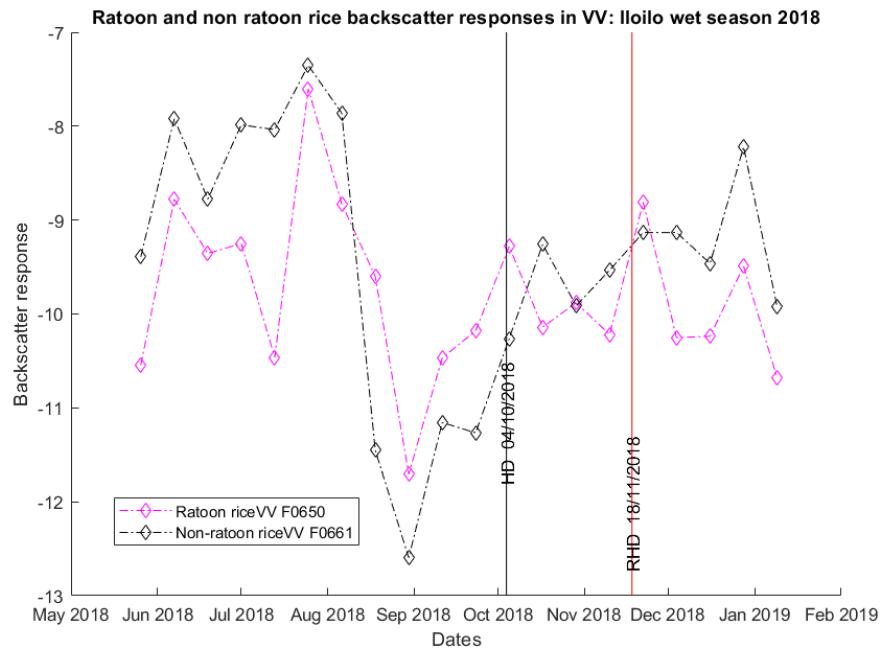


Figure 3.2: Temporal signature of ratoon (pink) and non-ratoon (black dotted) rice crop in VV polarisation in the study region of Iloilo during wet season 2018

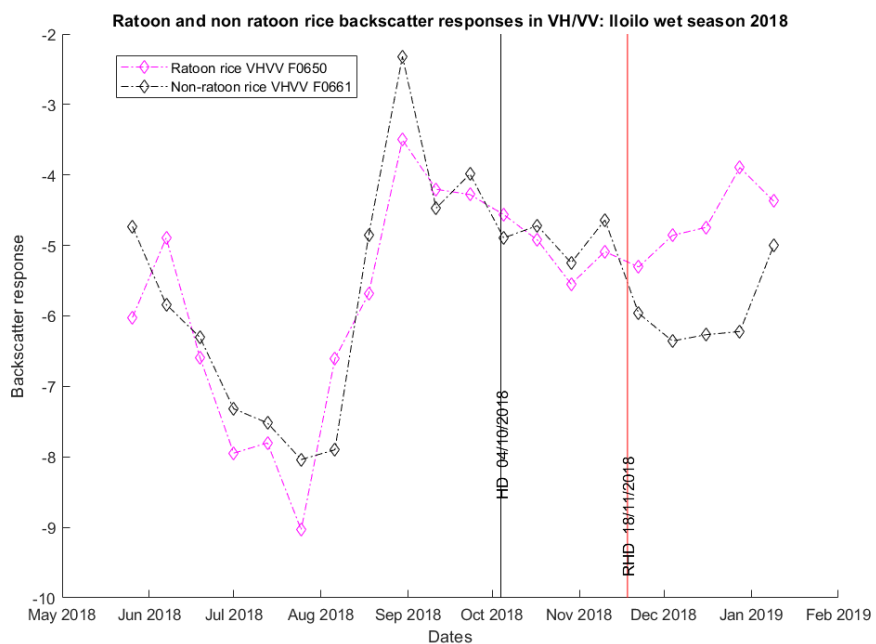


Figure 3.3: Temporal signature of ratoon (pink) and non-ratoon (black dotted) rice crop in VH/VV ratio polarisation in the study region of Iloilo during wet season 2018

Figures 3.1 to 3.3 show the temporal signature of ratoon (pink) and non-ratoon (black dotted) rice crops in VH, VV and VH/VV polarisation in the study region of Iloilo during wet season 2018. Vertical lines have been used for representing the harvesting dates of primary (HD) and ratoon (RCHD) rice crops.

3.2. Selection of ratoon and non-ratoon dataset for significance test

3.2.1. Sub-selection of ratoon dataset

Although the total ratoon samples in the selected provinces were 42 (Table 2.2), only 30 samples have been selected for performing significance U test and random forest classification; the main reasons for choosing these samples are following:

- Nine samples have been removed because of ratoon harvesting dates. The ratoon harvesting dates of these samples were predicted outside of the study period when no image data was available (April 2019).
- Three samples from Leyte and Agusan del Sur were removed because ratoon rice crop duration was very short, and backscatter data were insufficient to cover growth stages such as flowering and ripening.

Table 3.1 shows the criteria that have been used for selecting the growth stages in the ratoon crops. The growth stages of the ratoon crop are divided into three stages, including the short crop growth has 12-15 days of flowering and 25-30 days for ripening stages. On the other hand, a long duration of the crop is in the case flowering growth stage 25-30 days and ripening for 60-65 days.

Table 3.1: Selection of growth stages of ratoon rice crop

Growth criteria	Assumption of ratoon crop growth stages	Growth duration days for RS data selection
Immediately after harvest of primary crop	vegetative	3 -5 days after harvest of the primary crop
Based on ratoon crop duration*	flowering	Short- 12-15 days after the harvest of the primary crop in the ratoon field Longest - 25-30 days after the harvest of the primary crop in the ratoon field
Based on ratoon crop duration*	Ripening	Short - 25 -30 after the harvest of the primary crop in ratoon Longest -60-65 after the harvest

3.2.2. Selection of non-ratoon dataset

The selection of non-ratoon fields for testing and classification has been made based on the ratoon field. This means that the basic parameters such as harvested dates of the primary rice crop, method of harvesting and ecosystem of the crop had to be the same for selecting non-ratoon sample fields (see appendix 1). It has been highly balanced that the harvesting date of ratoon and non-ratoon with selected parameters (Table 3.3) must have gaps of 15-20 days. This helped to distinguish the difference between temporal backscatter responses between the ratoon non-ratoon rice crop after harvesting. In total, 30 non-ratoon samples have been selected to perform the statistical testing and RF classification with ratoon fields.

Table 3.2: Examples of parameters that were used for the selecting of non-ratoon fields

Non-ratoon		
Non-ratoonFID	Ecosystem	HarMethod
F0625_1	rainfed	mechanical
F0630_1	irrigated	manual
F0639_0	irrigated	manual
F0638_0	irrigated	mechanical
F0638_1	irrigated	Mechanical

3.3. Mean backscatter values in different growth stages using VV, VH and VH/VV polarisations

Table 3.3 shows the mean values of selected ratoon and non-ratoon samples at different growth stages in VV, VH and VH/VV polarisations. The mean values vary in each growing stage of the rice crop and different polarization. As such VV has a mean value of VV= -9.11, VH = -14.42. and VH/VV= -5.30 in ratoon rice crop while in the non- ratoon rice crop VV= -9.43, VH=-14.77 and VH/VV=-5.33 at the vegetative growth stages. Additionally, the flowering and ripening stages also show the different mean values. Ripening VH and ripening ratio are the only two groups where the mean difference is > 1db.

DETECTING RATOON RICE AND MAPPING ITS DISTRIBUTION USING MACHINE LEARNING ALGORITHM AND SENTINEL-1 TIME SERIES DATA

Table 3.3: Mean backscatter values of selected samples in VV, VH and VH/VV polarisations for ratoon and non-ratoon rice crop

Growth Stage	VV		VH		VH/VV	
	Ratoon	Non-ratoon	Ratoon	Non-Ratoon	Ratoon	Non-ratoon
Vegetative	-9.11	-9.43	-14.42	-14.77	-5.30	-5.33
Flowering	-9.21	-9.57	-14.49	-15.37	-5.27	-5.79
Ripening	-9.33	-10.20	-14.69	-16.88	-5.35	-6.68

Figures 3.4,3.5, and 3.6 show the boxplots of extracted mean values from Sentinel-1 time series data at different growth stages of ratoon and non-ratoon rice in VV, VH polarisations and VH/VV ratio. A total 30 samples for ratoon rice and 30 samples for non-ratoon rice crop has been plotted for VH (Figure 3.4), VV (Figure 3.5) and VH/VV ratio (Figure 3.6). The boxplots represent median as the tick horizontal middle line in the box, 25 percentiles as the lower half of the box, 75 percentile upper half of the box. Maximum and minimum values are represented as extent of the boxplot, and the black dots are interpreted as outliers of the boxplot.

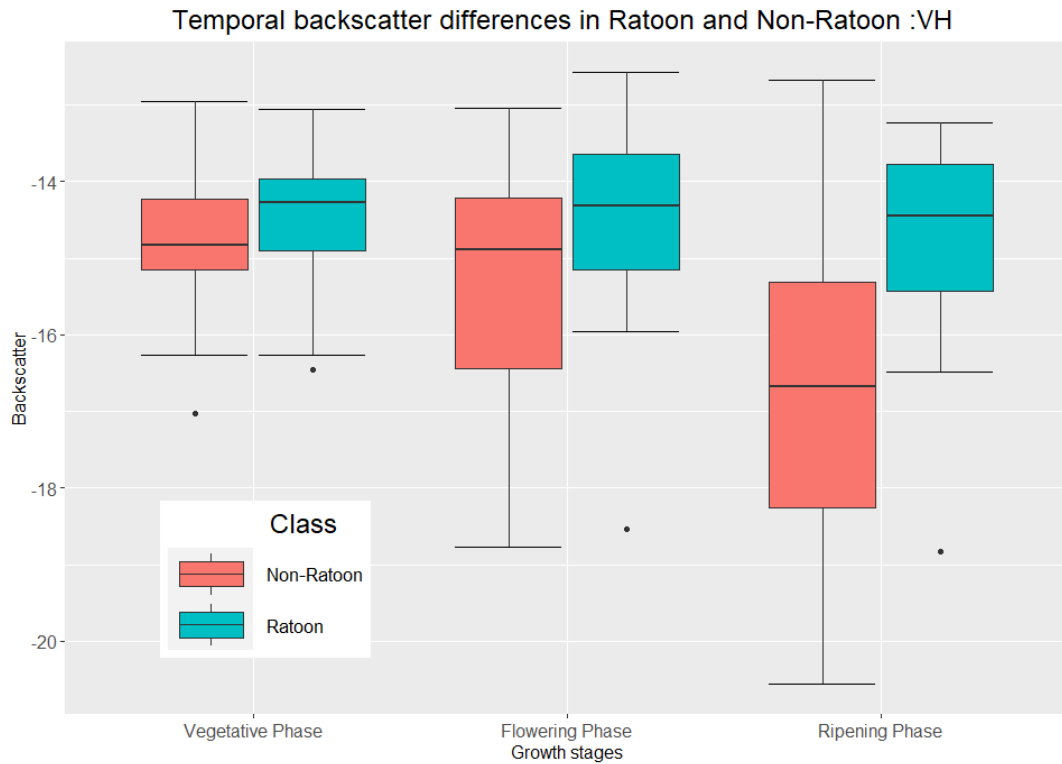


Figure 3.4: Box plot presenting the temporal backscatter variation in ratoon and- non-ratoon at different ratoon growth stages using VH (N= 60)

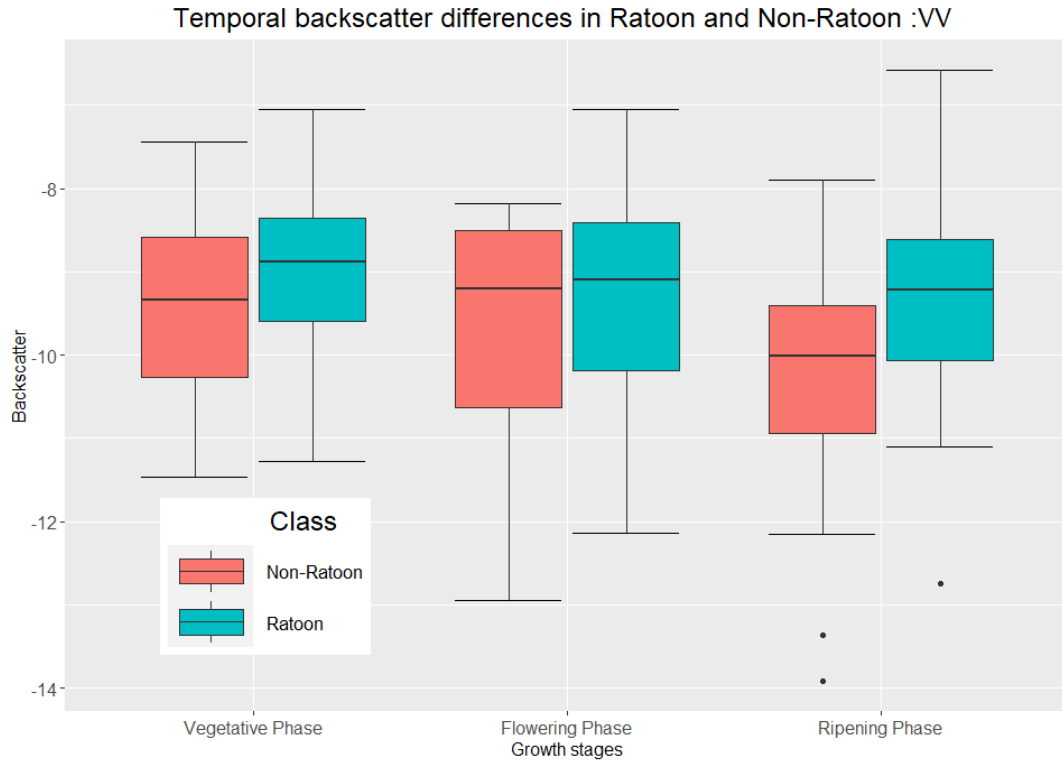


Figure 3.5: Box plot presenting the temporal backscatter variation in ratoon and non-ratoon at different ratoon growth stages using VV (N= 60)

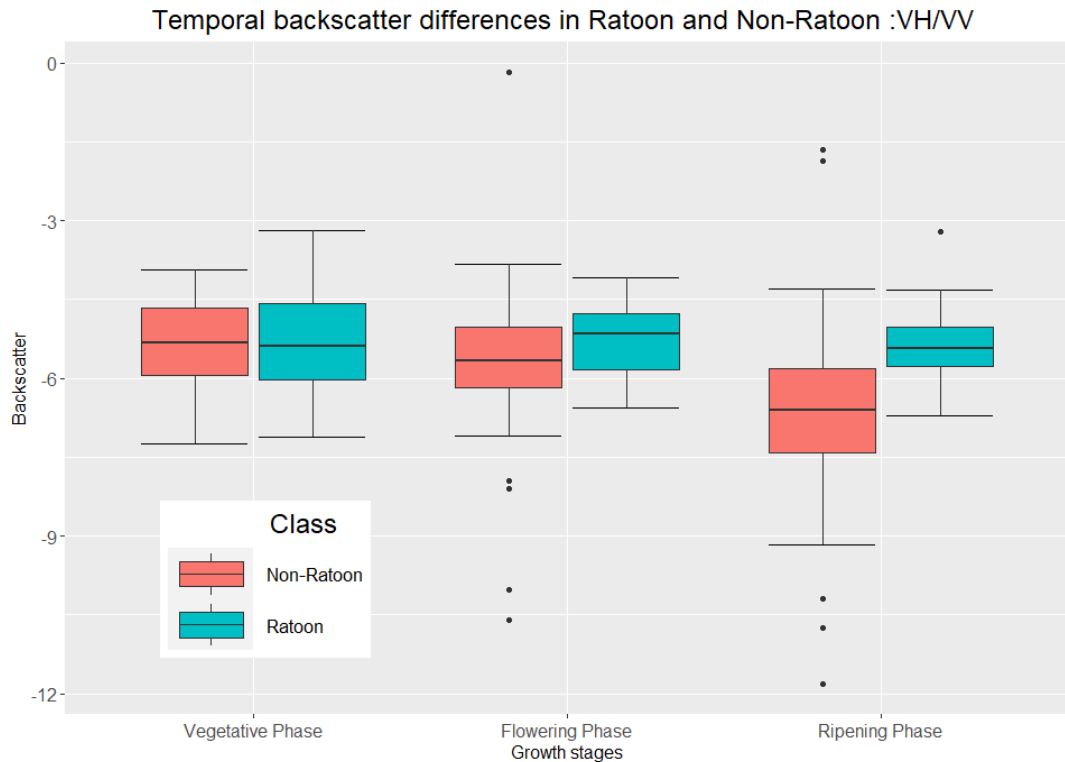


Figure 3.6: Box plot presenting the temporal backscatter variation in ratoon and non-ratoon at different ratoon growth stages using VH/VV (N= 60)

3.4. Mann-Whitney U test: Significance test

The significant differences between ratoon and non-ratoon crop testing are essential; that is why a Mann-Whitney U test has been selected to test the significance of temporal backscatter responses between ratoon and non-ratoon crops. Through significance test, backscatter information of ratoon and the non-ratoon crop has been taken as the independent variable. In contrast, ratoon and non-ratoon have been considered as categorical dependent variables. Table 3.5 shows p-values in ratoon and non-ratoon using VV, VH, and VH/VV polarisation at different growing stages. The p-value has been used for determining the significant between ratoon and non-ratoon rice. The p-values in different polarisations such as VV=0.198, VH= 0.065 and VH/VV= 0.976, which the vegetative stage is not significant. On the other hand, the ripening stage shows the significance between ratoon and non-ratoon rice crops in VV, VH and VH/VV polarisations. The p-values are 0.00 in VH and VH/VV, while 0.038 in VV polarisation.

Table 3.4: P -values from a Mann- Whitney U test in ratoon and non-ratoon rice crops using VV, VH, and VH/VV polarisations when ratoon crops are at growing stages (N= 60)

Growth Stage	VV	VH	VH/VV
Vegetation	0.198	0.065	0.976
Flowering	0.359	0.035	0.081
Ripening	0.038	0.000	0.000

3.5. Classification: Random forest

The R programming language has been used for random forest classification using ratoon and non-ratoon classes. Various packages and libraries (raster, rgdal, and caret) were used for classification. The confusion matrices for the trained model and prediction dataset have been generated using these libraries. Classification has been performed using VV, VH and VH/VV polarisations of sentinel-1 backscatter data. The backscatter data has been prepared following the growth stages of the ratoon rice crop (vegetation and flowering, and ripening) (Table 3.1). Ratoon and non-ratoon classes have an equal number of samples (each 30 samples), resulting in a total of 60 samples. The selection of samples for training and prediction data has been made automatically and randomly using the random forest model. The random forest model has been tuned for increasing the accuracy. The parameters such as ntree, mtry have been used for tuning the random forest model. The 300 ntree and 2 mtry have been applied to achieving the best accuracy from the model.

3.5.1. Confusion matrix: trained data model

The RF trained using ratoon and non-ratoon features, and the RF produced a confusion matrix and OOB error estimates. Table 3.5 shows the confusion matrix of the training dataset using VV, VH and VH/VV polarisations and, it shows the 38.39 % OOB estimates rates of the random forest model. The class error shows the misclassification in the RF model in table 3.7. The extend of class error is from 0 to 1. The higher the class error means more misclassification and represents the unfit model for use. On the other hand, the lower-class error means a higher chance for the correct classification of features. The class error in ratoon and non- ratoon classes are 0.450 and 0.338, respectively.

Table 3.5: Confusion matrix and OOB error rate of RF classifier for ratoon and non-ratoon classes using VV, VH and VH/VV polarisations (N= 60)

Reference				
Prediction	Ratoon	Non-Ratoon	Total	Class Error
Ratoon	33	27	60	0.45
Non-Ratoon	24	47	71	0.33
Total	57	74	131	

OOB estimate of error rate: 38.93%

3.5.2. Variable importance of the trained model

Table 3.6 demonstrates the important variables for the development of the RF classifier. The Gini index value determines the variable importance, and the higher the value is representing, the higher the importance value. The variable ranking was based on the mean decrease Gini value. The variable importance shows the mean decrease in impurity among the datasets. It splits in each tree and improves the split -criterion in the importance measure attributed to the split variable—Table 3.6 shows the important variable in different growing stages of ratoon and non-ratoon rice crops.

Table 3.6: Variable importance of the trained model

Growth Stage	VV	VH	VH/VV
Vegetation	8.52	4.77	6.84
Flowering	7.00	7.09	5.95
Ripening	4.09	9.36	6.58
Total	19.92	24.35	20.24

The integrated data of different growth stages are shown in Table 3.6 that VH (24.35) is an important variable than VV (19.92) and VH/VV (20.24). In addition, VV is a more important variable in the vegetative stage than VH and VH/VV, While VH scores higher Gini values at the flowering stage and ripening in the development of the RF.

3.5.3. Confusion matrices: Prediction data

The trained RF classifier was used with test data (1/3 or 30%) to assess non-ratoon and ratoon samples' classification accuracy overall and at each growth stage. Table 3.7 shows the overall classification accuracy

has been obtained 69.39 %, and the kappa value is 0.39 from the testing dataset. However, the accuracy at different growth stages varies, which are showing in table 3.8 to 3.10.

Table 3.7: Confusion matrix and obtained classification accuracies of ratoon and non-ratoon rice crops using prediction/test data

OA: overall accuracy, PA: producer accuracy and UA: user accuracy

Reference					
Prediction	Ratoon	Non-Ratoon	Total	PA (%)	UA (%)
Ratoon	19	4	23	63.33	82.60
Non-Ratoon	11	15	26	78.94	57.69
Total	30	19	49		
OA (%)	69.39				
Kappa	0.39				

3.5.4. Random forest classification with prediction dataset at different growing stages

Tables 3.8 to 3.10 show the confusion matrices of ratoon and non-ratoon rice crops at different stages such as vegetation, flowering and ripening of prediction data using VV, VH and VH/VV polarisations.

Table 3.8: Confusion matrix and obtained classification accuracies for non-ratoon and ratoon rice crops at vegetative stage using prediction data

OA: overall accuracy, PA: producer accuracy and UA: user accuracy

Reference					
Prediction	Ratoon	Non-Ratoon	Total	PA (%)	UA (%)
Ratoon	2	0	2	16.66	100.00
Non-Ratoon	10	6	16	100.00	37.50
Total	12	6	18		
OA (%)	44.44				
Kappa	0.11				

DETECTING RATOON RICE AND MAPPING ITS DISTRIBUTION USING MACHINE LEARNING ALGORITHM AND SENTINEL-1 TIME SERIES DATA

Table 3.8 shows the confusion matrix and obtained accuracy from the vegetative stage prediction dataset with ratoon and non-ratoon features in VV, VH, and VH/VV polarisation. The overall accuracy is obtained at 44.44% and kappa = 0.11.

Table 3.9: Confusion matrix and obtained classification accuracies for non-ratoon and ratoon rice crops at flowering stage using prediction/test data

OA: overall accuracy, **PA:** producer accuracy and **UA:** user accuracy

Reference					
Prediction	Ratoon	Non-Ratoon	Total	PA (%)	UA (%)
Ratoon	7	1	8	58.33	87.50
Non-Ratoon	5	5	10	83.33	50.00
Total	12	6	18		
OA (%)	66.67				
Kappa	0.35				

Table 3.9 shows the confusion matrix and obtained accuracy from the prediction dataset of the flowering stage with ratoon and non-ratoon features in VV, VH and, VH/VV polarisation. The overall accuracy is obtained at 66.67% and kappa = 0.35.

Table 3.10: Confusion matrix and obtained classification accuracies for non-ratoon and ratoon rice crops at ripening stage using prediction/test data

OA: overall accuracy, **PA:** producer accuracy and **UA:** user accuracy

Reference					
Prediction	Ratoon	Non-Ratoon	Total	PA (%)	UA (%)
Ratoon	8	3	11	66.66	72.72
Non-Ratoon	4	3	7	50.00	42.85
Total	12	6	18		
OA (%)	61.11				
Kappa	0.16				

Table 3.10 shows that confusion matrix and accuracy obtained using random forest classification at the ripening stage with VV, VH and VH/VV polarisations as ratoon and non-ratoon rice features. The overall accuracy is 61.00 %, and kappa = 0.16.

3.6. Distribution of ratoon and non-ratoon rice crop

The validated RF classification model was used to map ratoon and non-ratoon rice distribution based on field observation data. The Map showing the distribution of ratoon and non-ratoon of field observation during the study period 2017-2019 (Appendix IIIA, IIIB, and IIIC). Figures 3.7, 3.8 and 3.9 show the RF classification map of ratoon and non-ratoon rice crop for selected polygons from Leyte, Iloilo and Agusan del Sur province of the Philippines (See: Appendix IV for the province-based prediction map).

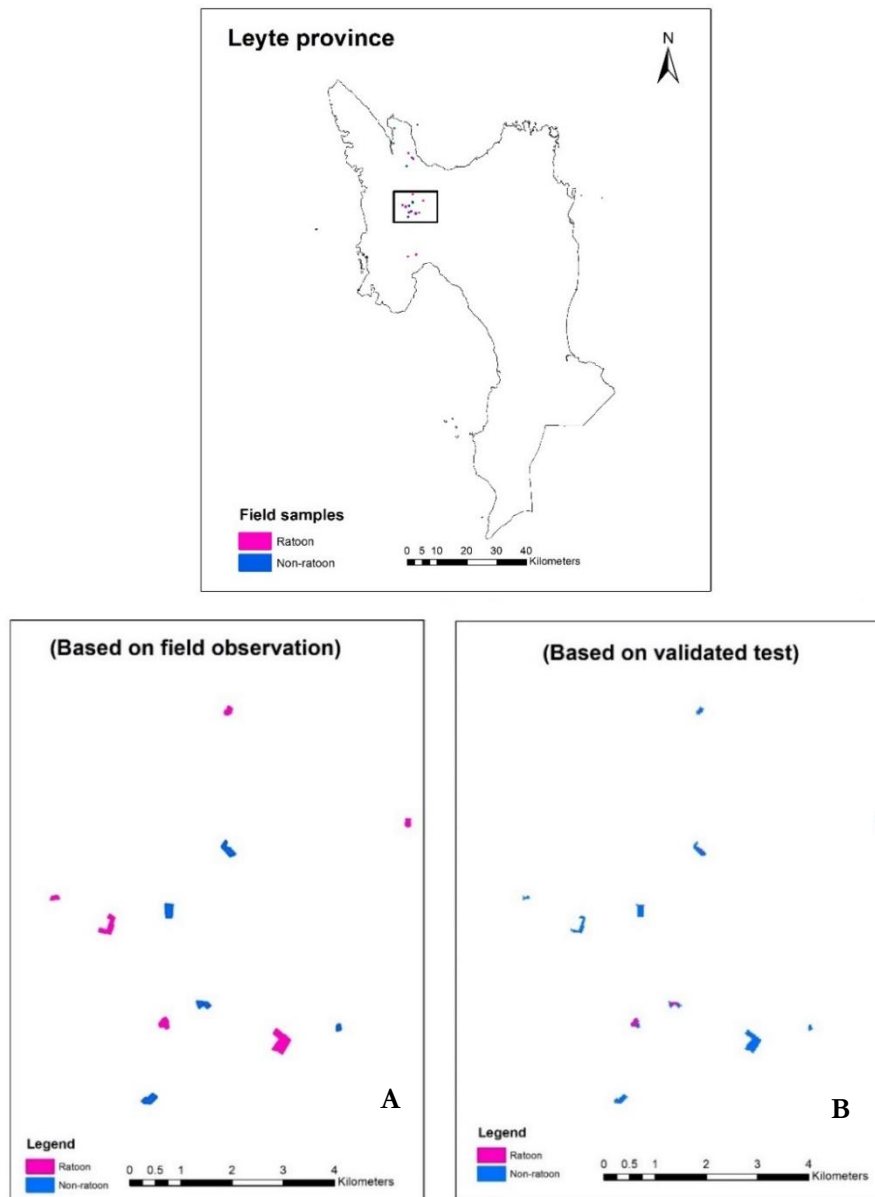


Figure 3.7: Map showing the distribution of ratoon and non-ratoon rice based on field observation and predicted classification of selected polygons from Leyte province

Figure 3.7 shows the field observation (A), and predicted classification (B) of ratoon and non-ratoon rice are shown in the Leyte province. The prediction classification is based on acquired Sentinel-1 imagery from 16-28 December 2018 using Google Earth Engine. The predicted and field observations of ratoon and non-ratoon rice crops are represented as pink and blue. The map shows that predicted ratoon and non-ratoon rice are not correctly classified because the maximum field observation (polygons) is blue, which shows non-ratoon rice.

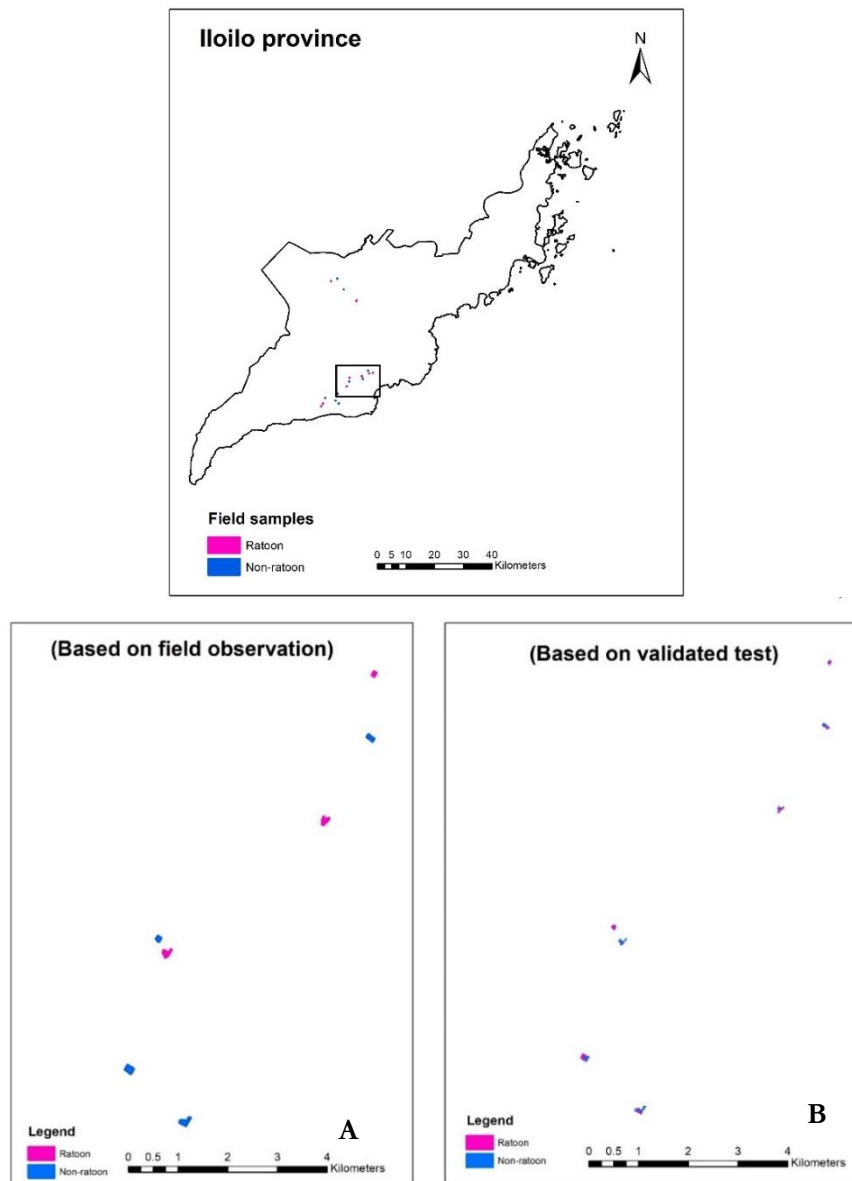


Figure 3.8: Map showing the distribution of ratoon and non-ratoon rice based on field observation and predicted classification of selected polygons from Iloilo province

Figure 3.8 shows the predicted (B) and field observation (A) ratoon and non-ratoon rice are presented in the Iloilo province. The prediction classification is based on acquired Sentinel-1 imagery from 16-28 December 2018 using Google Earth Engine. The predicted and field observations of ratoon and non-ratoon rice crops are represented as pink and blue. The map shows the misclassification of ratoon and non-ratoon rice in the predicted map.

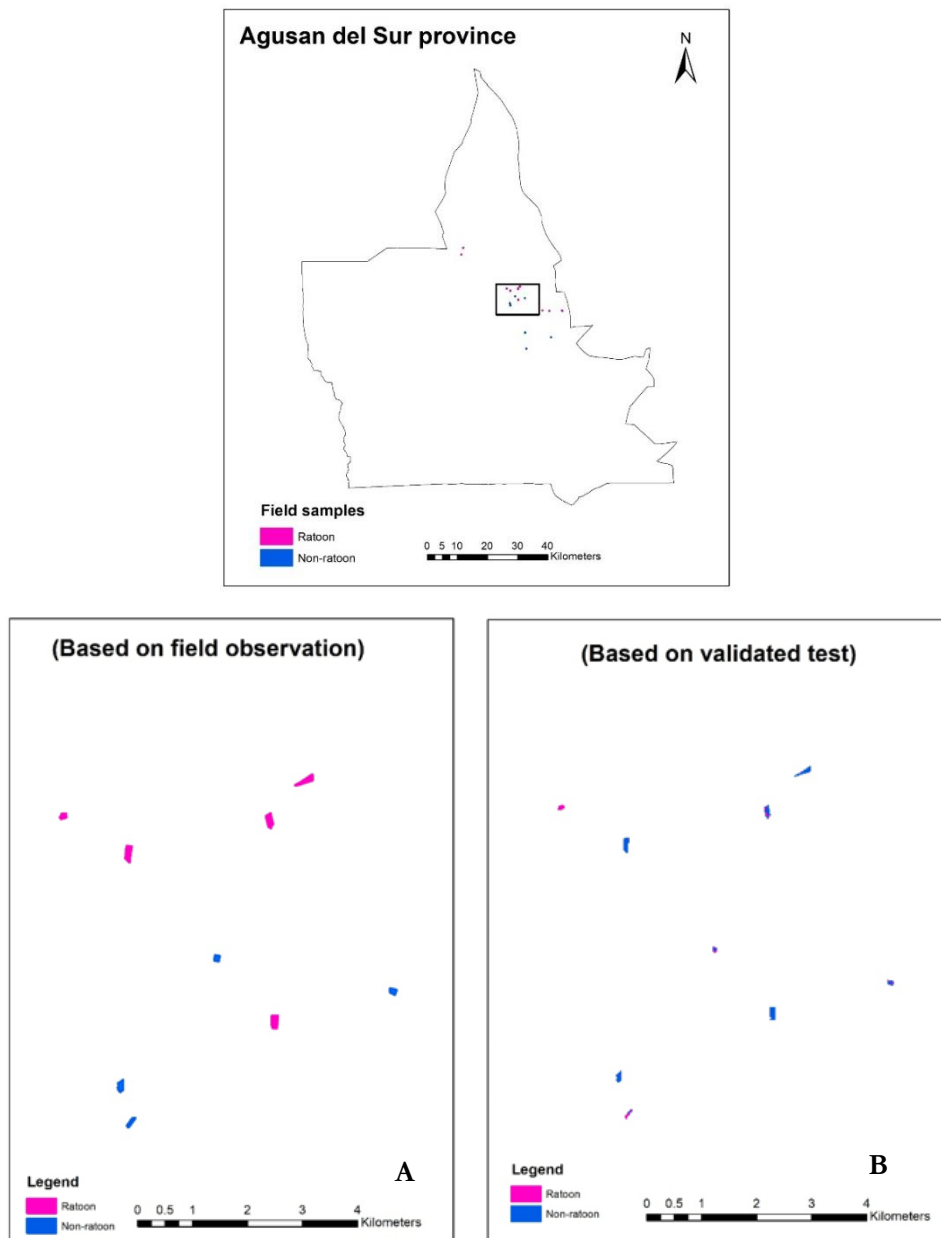


Figure 3.9: Map showing ratoon and non-ratoon rice distribution based on field observation and predicted classification of selected polygons from Agusan del Sur province.

Figure 3.9 shows the predicted (B) and field observation (A) ratoon and non-ratoon rice are presented in the Agusan del Sur province. The prediction classification is based on acquired Sentinel-1 imagery from 16-28 December 2018 using Google Earth Engine.

4. DISCUSSION

The estimation of rice production is essential because of continued high rates of consumption and increasing demand worldwide (Bandumula, 2018; Clauss et al., 2018). Thus, the distribution of rice as the primary crop has been mapped. Nevertheless, mapping ratoon rice has not gained much attention in the literature. There is a large research gap between the mapping and detection of ratoon and non-ratoon rice. In this study, ratoon and non-ratoon rice crop field samples were selected from the Leyte, Iloilo and Agusan del Sur province of the Philippines, collected during 2017-2019. This study evaluated that temporal backscatter signature from Sentinel-1 time-series data can differentiate between ratoon and non-ratoon rice fields by applying the Mann-Whitney U test. Finally, the RF model discriminated between the ratoon and non-ratoon rice at different growth stages and mapped its distribution. The important findings, limitations, and recommendations are discussed below.

4.1. Temporal backscattering behaviour of ratoon and non-ratoon rice in VV, VH and VH / VV polarisations

The temporal backscatter allows to explain crops phenological stages such as planting, flowering, ripening and harvesting (Harfenmeister et al., 2019). In our study, we used temporal backscatter data from Sentinel-1 time series data. To understand the difference in temporal backscatter of ratoon and non-ratoon rice crop, two field samples of ratoon and non-ratoon were selected from the Iloilo province. Both samples were plotted using VV, VH and VH/VV polarisations (Figure 3.1, 3.2 and 3.3). The results revealed that there were differences in temporal backscatter of ratoon and non-ratoon samples.

After harvesting the primary rice crop, the results showed differences in the temporal backscatter of ratoon and non-ratoon samples. This could be due to the harvesting methods determine the vegetation left on the field, height of the rice crop. Because when the ratoon is practised on the field, the crop was not entirely harvested from the surface, which meant the vegetation was left more than the non-ratoon field. In our analysis, we selected Sentinel-1 time series temporal backscatter data of 5 -10 days after harvesting the primary rice crop for the vegetation stage of ratoon rice. The ratio of mean backscatter value was smaller than 1dB (Table 3.4), even though that was counted as noise but no difference in ratoon and non-ratoon rice crop. There may be the closest difference in height and left vegetation on the field between the ratoon and non-ratoon rice crops.

The ratoon field requires flooding for growing vegetation again on the same harvested rice field after harvesting the primary rice crop (Oad et al., 2002). The flooding increases the vegetation, the intensity of the canopy and the height of the crop. In contrast, non-ratoon rice field becomes fallow land or preparing for other crops after harvesting. Sharifi & Hosseingholizadeh (2020) explained that the double bounce

backscattering influenced the backscatter of rice plant due to interaction with stem and surface water before reaching the flowering stage. The boxplot also presented differences in median values of backscatter in both crops using the VV, VH and VH/VV polarisations (Figure 3.5 and 3.6). Also, the ratio of ratoon and non-ratoon rice crops was close to one dB (0.94) at the flowering stage in VH, VH /VV polarisations. At the ripening stage, we found that VH polarisation and VH/VV ratio presented a large difference in median values of temporal backscatter (Figure 3.5 and 3.6). The difference between ratoon and non-ratoon was greater than 1dB (Table 3.3). The $dB > 1$ showed that there was a clear difference between ratoon and non-ratoon rice crops. The previous study by Dineshkumar & Satishkumar (2019) also explained that the temporal backscatter varied in the different growth of rice crop such as transplanting, flowering and grain mature in polarisations such as VV, VH and VH/VV polarisations., we analysed the means backscatter values in different stages like vegetative, flowering and ripening (Table 3.3). We found a clear difference in mean values of ratoon and non -ratoon rice crops in VH polarisation and VH/VV ratio at the ripening stage.

We used the Mann -Whitney U test to assess the significant difference between temporal backscatter data in ratoon and non -ratoon classes using VV, VH and VH/VV polarisations. The test result showed that at the vegetative phase, the mean backscatter of VV and VH polarisations was not significant. For instance, the vegetative stages presented result in VH ($p= 0.065$), VV($p=0.198$) and VH/VV ($p=0.976$) polarisation where P values >0.05 . The results at the flowering stages showed that p values were only significant in VH ($p =0.035$) and VH/VV ($p = 0.081$) polarisations (Table 3.4). In the last ripening stage, the p- values were significant in all polarisations VV (p-value=0.038), VH (p value=0.000) and VH/VV (p-value=0.000) (Table 3.4). We found that VH was significant when ratoon fields were at the flowering and ripening stages for differentiating ratoon and non-ratoon rice crops.

4.2. RF-based classification

Random forest (RF) based classification was performed to differentiate the ratoon and non-ratoon rice. The RF classifier calculated overall accuracy and kappa value from predicting the results. We divided the dataset into a 70/30 ratio for training and prediction results following Belgiu & Drăgu (2016) because the training and validation data must be statistically independent, large enough and presentative to each class. The RF obtained 69.39% overall accuracy (OA) and 0.39 kappa value applying the prediction dataset (Table 3.7). Landis & Koch (1977) indicated that kappa values range from 0.21–0.40 is classified as fair, which meant that model performance was acceptable for classification. Apart from the kappa and overall accuracy of the model, we also calculated the user and producer accuracy to evaluate the model's omission and commission errors. The user and producer accuracy of the RF model for ratoon rice was 82.60%, 63.33%, respectively, while the user and producer accuracy for non-ratoon was 57.69% and 78.94% (Table 3.7). Bazzi et al. (2019) also used the Sentinel-1 data-based RF model to map rice and other crops in the Camargue region, southern

France. They found a user, producer, overall accuracy, and kappa of 88.3%, 95.25, 96.6% and 87.5%, respectively. The user accuracy of this study was similar with Bazzi et al. (2019) finding ,whereas the other parameters showed a different results.

The RF model was also used to classify ratoon and non- ratoon rice crops at different growth stages (Table 3.8, 3.9 and 3.10). The lowest overall classification accuracy was found at the vegetative growth stage of ratoon rice compared to flowering and ripening stages. After harvesting, both ratoon and non- ratoon rice could have the same biomass (Table 3.3), it could have a similar backscatter. It could create confusion for the RF model to classify the classes correctly. On the other hand, at the flowering and ripening stages, the overall accuracy was 66.67% and 61.11%. Furthermore, the estimated OBB error rate at vegetative, flowering and ripening was 61.90%, 28.57% and 23.81%, respectively (Appendix IIA, IIB and IIC). The higher OBB error rate at the vegetative stage was due to the misclassification of ratoon rice class to non-ratoon rice class and vice versa.

The distribution of predicted ratoon and non-ratoon rice crops was estimated by using the RF model. The field samples and selected polygons from the Iloilo, Leyte and Agusan del Sur provinces of the Philippines were applied to validate the RF model (Figure 3.7, 3.8 and 3.9).

4.3. Limitations

In the following, we emphasised the study's limitations that constrain the scope to which the outcomes can be generalised further than the study restrictions.

- **Limitation of field surveyed and remote sensing data:** since we had missed many data of ratoon rice crop after its harvesting, i.e., April and May 2019 (dry season), we could only analyse the temporal backscatter behaviour of ratoon till March 2019; hence it makes the samples insufficient.
- **Limitation of sample size:** the field samples were are few for ratoon rice crops. It would be much better if there were more samples, like 100 samples and because the small sample size may produce inaccurate accuracies of detecting ratoon and non- ratoon rice crops.
- **Information of ratoon samples:** Ratoon rice samples did not observe thoroughly as primary rice crops had collected during the field survey. Furthermore, the Ratoon rice practice depends on farmers' decisions; for instance, it was challenging to conclude that they will practice ratoon rice seasonally on the same field. This limited the analysis between ratoon and non- ratoon rice crops in the study area.

4.4. Recommendations

Based on the results of this study, we propose some recommendations that can be applied for future work regarding the SAR dataset for detecting ratoon rice and its distribution:

1. The field survey can be performed separately for the ratoon rice crop because this crop is also essential and needs more information like primary rice crop. The sample size of the ratoon rice crop can be increased for more advanced study.
2. Other SAR satellites, such as RADARSAT-2 (band -C), PALSAR (L-band) and TerraSAR -X (band -X with high spatial-temporal resolution can also use for detecting ratoon rice like Sentinel-1.
3. The functional capability with a large dataset, proficiency in crop classification makes the RF model for selection in this study, while some other supervised machine learning classifiers such as SVM can be a different choice for detecting ratoon rice.

5. CONCLUSION

The study has shown the possibility of using the Sentinel-1 time series data for detecting ratoon and non-ratoon rice crops using VV, VH and VH/ VV polarisations. The two research hypotheses proposed in this study were (1) There is a significant difference in the temporal backscatter behaviour of rice and ratoon rice in different polarisation. (2) Ratoon rice can be accurately discriminated using a random forest (RF) algorithm, and Sentinel-1 time-series data have been examined and confirmed to be true. This study was performed using field survey data collected in 2017-2019 in three provinces of the Philippines: Leyte, Iloilo and Agusan del Sur. We selected ratoon and non- ratoon samples from the field survey data and defined the parameters to consider the ratoon growth stages, for instance, vegetative, flowering and ripening. We utilised Sentinel-1 time-series data to differentiate temporal backscatter information of ratoon and non- ratoon rice crops. The study defined ratoon rice growth stages for detecting the discrimination between ratoon and non-ratoon rice crops. A Mann -Whitney U test found significant differences in temporal backscatter of ratoon and non- ratoon rice for some stages of ratoon and non- ratoon rice crops. It found that p- values at vegetative were not significant while flowering and ripening were significant. We also differentiated the temporal backscattering of ratoon and non- ratoon rice.

Furthermore, we also performed a random forest classifier for ratoon and non- ratoon classification at different stages with predicting data set—the overall accuracy and kappa value utilized for comparing the result at various stages. The RF model obtained 69.39% overall accuracy from the prediction dataset, and the training dataset estimated 38.93% OBB error rate. In addition, the RF classification also applied to different growing stages of ratoon and on ratoon crop data. Furthermore, the RF model proved that ratoon and non- ratoon could be classified using time series Sentinel-1 data, and the RF model can achieve high accuracy. Finally, we applied a validated RF model for mapping ratoon rice in the Iloilo, Leyte, and Agusan del Sur provinces in the Philippines.

Furthermore, the random forest classifier can detect ratoon and non -ratoon rice. Rice mapping using SAR data has been performing at a large scale since the 1990s, and ratoon rice mapping has been given less attention. This study can help the research community explore the potential values using more Sentinel-1 SAR data to map the ratoon rice area and its distribution.

6. LIST OF REFERENCES

- Alonso-González, A., & Hajnsek, I. (2019). Radar Remote Sensing of Land Surface Parameters. https://doi.org/10.1007/978-3-662-48297-1_12
- Aschbacher, J., Pongsrihadulchai, A., Karnchanasutham, S., Rodprom, C., Paudya, D. R., & Toan, T. Le. (1995). Assessment of ERS-1 SAR data for rice crop mapping and monitoring. 83–85.
- Aung, Y. Y., & Min, M. M. (2017). An analysis of random forest algorithm-based network intrusion detection system. Proceedings - 18th IEEE/ACIS International Conference on Software Engineering, Artificial Intelligence, Networking and Parallel/Distributed Computing, SNPD 2017, 127–132. <https://doi.org/10.1109/SNPD.2017.8022711>
- Ayele, G. T., Tebeje, A. K., Demissie, S. S., Belete, M. A., Jemberrie, M. A., Teshome, W. M., Mengistu, D. T., & Teshale, E. Z. (2018). Time series land cover mapping and change detection analysis using geographic information system and remote sensing, Northern Ethiopia. Air, Soil and Water Research, 11. <https://doi.org/10.1177/1178622117751603>
- Baghdadi, N., Boyer, N., Todoroff, P., El Hajj, M., & Bégué, A. (2009). Potential of SAR sensors TerraSAR-X, ASAR/ENVISAT and PALSAR/ALOS for monitoring sugarcane crops on Reunion Island. Remote Sensing of Environment, 113(8), 1724–1738. <https://doi.org/10.1016/j.rse.2009.04.005>
- Bandumula, N. (2018). Rice Production in Asia: Key to Global Food Security. Proceedings of the National Academy of Sciences India Section B - Biological Sciences, 88(4), 1323–1328. <https://doi.org/10.1007/s40011-017-0867-7>
- Bazzi, H., Baghdadi, N., El Hajj, M., Zribi, M., Minh, D. H. T., Ndikumana, E., Courault, D., & Belhouchette, H. (2019). Mapping paddy rice using Sentinel-1 SAR time series in Camargue, France. Remote Sensing, 11(7), 1–16. <https://doi.org/10.3390/RS11070887>
- Bégué, A., Arvor, D., Bellon, B., Betbeder, J., de Abelleira, D., Ferraz, R. P. D., Lebourgeois, V., Lelong, C., Simões, M., & Verón, S. R. (2018). Remote sensing and cropping practices: A review. Remote Sensing, 10(1). <https://doi.org/10.3390/rs10010099>
- Belgiu, M., & Drăgu, L. (2016). Random forest in remote sensing: A review of applications and future directions. In ISPRS Journal of Photogrammetry and Remote Sensing (Vol. 114, pp. 24–31). <https://doi.org/10.1016/j.isprsjprs.2016.01.011>
- Benedict A. Exconde. (2016). Rice Production and Consumption Trends in the Philippines from 2000 to 2015. In Yuchengco Center.
- Breiman, L. (1999). Random Forests - Random Features, Technical Report 567, Statistic Department, University of California, Berkeley, (<https://www.stat.berkeley.edu/~breiman/random-forests.pdf>, 08.10.2018'de erişildi). 1–29.
- Breiman, L. (2001). Random forests. Machine Learning. <https://doi.org/10.1023/A:1010933404324>
- Breiman, L., Freidman, J. H., Olshen, R. A., & Stone, C. J. (1984). Classification and Regression Trees. Chapman & Hall/CRC Taylor & Francis Group 6000 Broken Sound Parkway NW, Suite 300 Boca Raton, FL 33487-2742.
- Brodley, C. E., & Friedl, M. A. (1997). Decision tree classification of land cover from remotely sensed data. Remote Sensing of Environment, 61(3), 399–409. [https://doi.org/10.1016/S0034-4257\(97\)00049-7](https://doi.org/10.1016/S0034-4257(97)00049-7)
- Cai, Y., Lin, H., & Zhang, M. (2019). Mapping paddy rice by the object-based random forest method using time series Sentinel-1/Sentinel-2 data. Advances in Space Research, 64(11), 2233–2244. <https://doi.org/10.1016/j.asr.2019.08.042>

- Chauhan, B. S., Awan, T. H., Abugho, S. B., & Evengelista, G. (2015). Effect of crop establishment methods and weed control treatments on weed management and rice yield. *Field Crops Research*, 172, 72–84. <https://doi.org/10.1016/j.fcr.2014.12.011>
- Chen, Q., He, A., Wang, W., Peng, S., Huang, J., Cui, K., & Nie, L. (2018). Comparisons of regeneration rate and yields performance between inbred and hybrid rice cultivars in a direct seeding rice-ratoon rice system in central China. *Field Crops Research*, 223(January), 164–170. <https://doi.org/10.1016/j.fcr.2018.04.010>
- Clauss, K., Ottinger, M., & Kuenzer, C. (2018). Mapping rice areas with Sentinel-1 time series and superpixel segmentation. *International Journal of Remote Sensing*, 39(5), 1399–1420. <https://doi.org/10.1080/01431161.2017.1404162>
- Coronas, J., & Philippines. (1920). The climate and weather of the Philippines, 1903-1918 (p. 195). Bureau of Printing. <file://catalog.hathitrust.org/Record/001486256>
- Dawe, D. (2013). Geographic determinants of rice self-sufficiency in Southeast Asia. *ESA Working Paper*, No. 13-03(13), 1–17.
- Dineshkumar, C., & Satishkumar, J. (2019). Rice crop monitoring using sentinel-1 C-band data. *International Archives of the Photogrammetry, Remote Sensing and Spatial Information Sciences - ISPRS Archives*, 42(3/W6), 73–77. <https://doi.org/10.5194/isprs-archives-XLII-3-W6-73-2019>
- Doering, O., & Sorensen, A. (2018). The land that shapes and sustains us. *How to Feed the World*, 46–58. <https://doi.org/10.5822/978-1-61091-885-5>
- FAOSTAT.(2020.). Retrieved 25 October 2020, from http://www.fao.org/faostat/en/#rankings/countries_by_commodity
- Faruq, G., Taha, R. M., & Prodhan, Z. H. (2014). Rice ratoon crop: A sustainable rice production system for tropical hill agriculture. *Sustainability (Switzerland)*, 6(9), 5785–5800. <https://doi.org/10.3390/su6095785>
- Feng, W., Sui, H., Tu, J., Huang, W., & Sun, K. (2018). A novel change detection approach based on visual saliency and random forest from multi-temporal high-resolution remote-sensing images. *International Journal of Remote Sensing*, 39(22), 7998–8021. <https://doi.org/10.1080/01431161.2018.1479794>
- Fikriyah, V. N., Darvishzadeh, R., Laborte, A., Khan, N. I., & Nelson, A. (2019). Discriminating transplanted and direct-seeded rice using Sentinel-1 intensity data. *International Journal of Applied Earth Observation and Geoinformation*, 76(June 2018), 143–153. <https://doi.org/10.1016/j.jag.2018.11.007>
- Geudtner, D., Torres, R., Snoeij, P., & Davidson, M. (2012). Sentinel-1 System Overview. In 9th European Conference on Synthetic Aperture Radar.
- Geudtner, D., Torres, R., Snoeij, P., Davidson, M., & Rommen, B. (2014). Sentinel-1 System capabilities and applications. *International Geoscience and Remote Sensing Symposium (IGARSS)*, 1457–1460. <https://doi.org/10.1109/IGARSS.2014.6946711>
- Han, L., Yang, G., Dai, H., Xu, B., Yang, H., Feng, H., Li, Z., & Yang, X. (2019). Modelling maize above-ground biomass based on machine learning approaches using UAV remote-sensing data. *Plant Methods*, 15(1), 1–19. <https://doi.org/10.1186/s13007-019-0394-z>
- Harfenmeister, K., Spengler, D., & Weltzien, C. (2019). Analysing temporal and spatial characteristics of crop parameters using Sentinel-1 backscatter data. *Remote Sensing*, 11(13), 1–30. <https://doi.org/10.3390/rs11131569>
- Im, J., Park, S., Rhee, J., Baik, J., & Choi, M. (2016). Downscaling of AMSR-E soil moisture with MODIS products using machine learning approaches. *Environmental Earth Sciences*, 75(15), 1–19. <https://doi.org/10.1007/s12665-016-5917-6>
- Inoue, Y., Sakaiya, E., & Wang, C. (2014). Capability of C-band backscattering coefficients from high-resolution satellite SAR sensors to assess biophysical variables in paddy rice. *Remote Sensing of Environment*, 140, 257–266. <https://doi.org/10.1016/j.rse.2013.09.001>

- IRRI, (1998). RICE RATOONING (p. 280). International Rice Research Institute (IRRI).
- Ishitsuka, N. (2018). Identification of paddy rice areas using SAR: Some case studies in Japan. *Japan Agricultural Research Quarterly*, 52(3), 197–204. <https://doi.org/10.6090/jarq.52.197>
- Janitza, S., & Hornung, R. (2018). On the overestimation of random forest's out-of-bag error. In *PLoS ONE* (Vol. 13, Issue 8). <https://doi.org/10.1371/journal.pone.0201904>
- Joshi, N., Baumann, M., Ehammer, A., Fensholt, R., Grogan, K., Hostert, P., Jepsen, M. R., Kuemmerle, T., Meyfroidt, P., Mitchard, E. T. A., Reiche, J., Ryan, C. M., & Waske, B. (2016). A review of the application of optical and radar remote sensing data fusion to land use mapping and monitoring. *Remote Sensing*, 8(1), 1–23. <https://doi.org/10.3390/rs8010070>
- Karthikeyan, L., Chawla, I., & Mishra, A. K. (2020). A review of remote sensing applications in agriculture for food security: Crop growth and yield, irrigation, and crop losses. *Journal of Hydrology*, 586(March), 124905. <https://doi.org/10.1016/j.jhydrol.2020.124905>
- Kavzoglu, T., & Mather, P. M. (2003). The use of backpropagating artificial neural networks in land cover classification. *International Journal of Remote Sensing*, 24(23), 4907–4938. <https://doi.org/10.1080/0143116031000114851>
- Krishnamurthy, K. (1989). Rice ratooning as an alternative to double cropping in tropical Asia. IRRI.
- Lam-Dao, N., Apan, A., Young, F., Le-Van, T., Le-Toan, T., & Bouvet, A. (2007). Rice monitoring using ENVISAT ASAR data: Preliminary results of a case study in the Mekong River Delta, Vietnam. 28th Asian Conference on Remote Sensing 2007, ACRS 2007, 1(January), 21–27.
- Landicho, L. D., Paelmo, R. F., Cabahug, R. D., de Luna, C. C., Visco, R. G., & Tolentino, L. L. (2016). Climate change adaptation strategies of smallholder agroforestry farmers in the Philippines. *Journal of Environmental Science and Management*, 19(1), 37–45.
- Landis, J. R., & Koch, G. G. (1977). The measurement of observer agreement for categorical data. *Biometrics*, 33(1), 159–174.
- Lasko, K., Vadrevu, K. P., Tran, V. T., & Justice, C. (2018). Mapping Double and Single Crop Paddy Rice with Sentinel-1A at Varying Spatial Scales and Polarizations in Hanoi, Vietnam. *IEEE Journal of Selected Topics in Applied Earth Observations and Remote Sensing*, 11(2), 498–512. <https://doi.org/10.1109/JSTARS.2017.2784784>
- Li, M., Zang, S., Zhang, B., Li, S., & Wu, C. (2014). A review of remote sensing image classification techniques: The role of Spatio-contextual information. *European Journal of Remote Sensing*, 47(1), 389–411. <https://doi.org/10.5721/EuJRS20144723>
- Liu, K. Lou, Li, Y. Z., & Hu, H. W. (2015). Predicting Ratoon rice growth rhythm based on NDVI at key growth stages of main rice. *Chilean Journal of Agricultural Research*, 75(4), 410–417. <https://doi.org/10.4067/S0718-58392015000500005>
- Liu, S., Chen, Y., Ma, Y., Kong, X., Zhang, X., & Zhang, D. (2020). Mapping Ratoon Rice Planting Area in Central China Using Sentinel-2 Time Stacks and The Phenology-Based Algorithm. *Remote Sensing*, 12(20), 3400. <https://doi.org/10.3390/rs12203400>
- Misra, G., Kumar, A., Patel, N. R., & Zurita-Milla, R. (2014). Mapping a Specific Crop-A Temporal Approach for Sugarcane Ratoon. *Journal of the Indian Society of Remote Sensing*, 42(2), 325–334. <https://doi.org/10.1007/s12524-012-0252-1>
- Miyaoka, K., Maki, M., Susaki, J., Homma, K., Yoshida, K., & Hongo, C. (2012). Detection of rice-planted area using multi-temporal ALOS / PALSAR data graduate school of engineering, Kyoto University Graduate School of Agriculture, Kyoto University College of Agriculture, Ibaraki University Center for Environmental Remote Sensing. 1, 6777–6780.
- Negalur, R. B., Yadahalli, G. S., Chittapur, B. M., Guruprasad, G. S., & Narappa, G. (2017). Ratoon Rice: A Climate and Resource Smart Technology. *International Journal of Current Microbiology and Applied Sciences*, 6(5), 1638–1653. <https://doi.org/10.20546/ijcmas.2017.605.179>

- Nelson, A., Setiyono, T., Rala, A. B., Quicho, E. D., Raviz, J. V., Abonete, P. J., Maunahan, A. A., Garcia, C. A., Bhatti, H. Z. M., Villano, L. S., Thongbai, P., Holecz, F., Barbieri, M., Collivignarelli, F., Gatti, L., Quilang, E. J. P., Mabalay, M. R. O., Mabalot, P. E., Barroga, M. I., ... Ninh, N. H. (2014). Towards an operational SAR-based rice monitoring system in Asia: Examples from 13 demonstration sites across Asia in the RIICE project. *Remote Sensing*, 6(11), 10773–10812. <https://doi.org/10.3390/rs61110773>
- Nguyen, D. B., & Wagner, W. (2017). European rice cropland mapping with Sentinel-1 data: The Mediterranean region case study. *Water (Switzerland)*, 9(6), 1–9. <https://doi.org/10.3390/w9060392>
- Oad, F.C., Cruz, P. S., Memon, N., Oad, N. L., & Zia-Ul-Hassan. (2002). Rice Ratooning Management. *Journal of Applied Sciences*, 2(1), 29–35. <https://doi.org/10.3923/jas.2002.29.35>
- Ozden, A., Faghri, A., Li, M., & Tabrizi, K. (2016). Evaluation of Synthetic Aperture Radar Satellite Remote Sensing for Pavement and Infrastructure Monitoring. *Procedia Engineering*, 145, 752–759. <https://doi.org/10.1016/j.proeng.2016.04.098>
- Pal, M. (2005). Random forest classifier for remote sensing classification. *International Journal of Remote Sensing*, 26(1), 217–222. <https://doi.org/10.1080/01431160412331269698>
- Panigrahy, S., Manjunath, K. R., Chakraborty, M., Kundu, N., & Parihar, J. S. (1999). Evaluation of RADARSAT Standard Beam data for identification of potato and rice crops in India. *ISPRS Journal of Photogrammetry and Remote Sensing*, 54(4), 254–262. [https://doi.org/10.1016/S0924-2716\(99\)00020-9](https://doi.org/10.1016/S0924-2716(99)00020-9)
- Raviz, J., Laborte, A., Barbieri, M., Mabalay, M. R., Garcia, C., Bibar, J. E. A., Mabalot, P., & Gonzaga, H. (2016). Mapping and monitoring rice areas in Central Luzon, Philippines using X and C-band SAR imagery. 37th Asian Conference on Remote Sensing, ACRS 2016, 1(December), 192–201.
- Saini, R., & Ghosh, S. K. (2018). Crop Classification on Single Date Sentinel-2 Imagery Using Random Forest and Support Vector Machine. *ISPRS - International Archives of the Photogrammetry, Remote Sensing and Spatial Information Sciences*, XLII-5(November), 683–688. <https://doi.org/10.5194/isprs-archives-xlii-5-683-2018>
- Santos, A. B., Fageria, N. K., & Prabhu, A. S. (2003). Rice ratooning management practices for higher yields. *Communications in Soil Science and Plant Analysis*, 34(5–6), 881–918. <https://doi.org/10.1081/CSS-120018981>
- Setiawan, A., Tyasmoro, S. Y., & Nugroho, A. (2014). Intermittent irrigation and cutting height on growth and yield ratoon rice (*Oryza sativa* L.). *Agrivita*, 36(1), 72–80.
- Shamiul Islam, M., Hasanuzzaman, M., & Rokonuzzaman, M. (2008). Ratoon rice response to different fertiliser doses in irrigated conditions. *Agriculturae Conspectus Scientificus*, 73(4), 197–202.
- Sharifi, A., & Hosseingholizadeh, M. (2020). Application of Sentinel-1 Data to Estimate Height and Biomass of Rice Crop in Astaneh-ye Ashrafiyeh, Iran. *Journal of the Indian Society of Remote Sensing*, 48(1), 11–19. <https://doi.org/10.1007/s12524-019-01057-8>
- Singha, M., Dong, J., Zhang, G., & Xiao, X. (2019). High-resolution paddy rice maps in cloud-prone Bangladesh and Northeast India using Sentinel-1 data. *Scientific Data*, 6(1), 1–10. <https://doi.org/10.1038/s41597-019-0036-3>
- Singla, S. K., Garg, R. D., & Dubey, O. P. (2018). Sugarcane ratoon discrimination using LANDSAT NDVI temporal data. *Spatial Information Research*, 26(4), 415–425. <https://doi.org/10.1007/s41324-018-0184-0>
- Son, N. T., Chen, C. F., Chen, C. R., & Minh, V. Q. (2018). Assessment of Sentinel-1A data for rice crop classification using random forests and support vector machines. *Geocarto International*, 33(6), 587–601. <https://doi.org/10.1080/10106049.2017.1289555>
- Story, M., & Congalton, R. G. (1986). Remote Sensing Brief Accuracy Assessment: A User's Perspective. *Photogrammetric Engineering and Remote Sensing*, 52(3), 397–399.
- Suga, Y., Takeuchi, S., Oguro, Y., & Konishi, T. (2000). Monitoring of rice-planted areas using space-borne

- SAR data. *International Archives of Photogrammetry and Remote Sensing*, XXXIII(Part B7), 1480–1483. http://www.isprs.org/proceedings/XXXIII/congress/part7/1480_XXXIII-part7.pdf
- Sun, C., Bian, Y., Zhou, T., & Pan, J. (2019). Using of Multi-Source and Multi-Temporal Remote Sensing Data Improves Crop-Type Mapping in the Subtropical Agriculture Region. *Sensors*, 19(10), 2401. <https://doi.org/10.3390/s19102401>
- Tibao, N. Y. (2009). Why Does the Philippines Import Rice : A Solution to the Rice Shortage. The 9th International Students Summit on Food, Agriculture, and Environment in the New Century, 1–4. http://www.nodai.ac.jp/cip/iss/english/9th_iss/fullpaper/1-1-5nchu-tibao.pdf
- Torbick, N., Chowdhury, D., Salas, W., & Qi, J. (2017). Monitoring Rice Agriculture across Myanmar Using Time Series Sentinel-1 Assisted by Landsat-8 and PALSAR-2. *Remote Sensing*, 9(2), 119. <https://doi.org/10.3390/rs9020119>
- Vapnik, V., & Cortes, C. (1995). Support-Vector Networks. *Machine Learning*, 20, 273–297. <https://doi.org/10.1109/64.163674>
- Vollset, S. E., Goren, E., Yuan, C. W., Cao, J., Smith, A. E., Hsiao, T., Bisignano, C., Azhar, G. S., Castro, E., Chalek, J., Dolgert, A. J., Frank, T., Fukutaki, K., Hay, S. I., Lozano, R., Mokdad, A. H., Nandakumar, V., Pierce, M., Pletcher, M., ... Murray, C. J. L. (2020). Fertility, mortality, migration, and population scenarios for 195 countries and territories from 2017 to 2100: a forecasting analysis for the Global Burden of Disease Study. *The Lancet*, 1–22. [https://doi.org/10.1016/S0140-6736\(20\)30677-2](https://doi.org/10.1016/S0140-6736(20)30677-2)
- Wang, W., He, A., Jiang, G., Sun, H., Jiang, M., Man, J., Ling, X., Cui, K., Huang, J., Peng, S., & Nie, L. (2020). Ratoon rice technology: A green and resource-efficient way for rice production. In *Advances in Agronomy* (1st ed., Vol. 159). Elsevier Inc. <https://doi.org/10.1016/bs.agron.2019.07.006>
- Yang, H., Pan, B., Wu, W., & Tai, J. (2018). Field-based rice classification in Wuhua county through integration of multi-temporal Sentinel-1A and Landsat-8 OLI data. *International Journal of Applied Earth Observation and Geoinformation*, 69(December 2017), 226–236. <https://doi.org/10.1016/j.jag.2018.02.019>
- Yap, B. W., & Sim, C. H. (2011). Comparisons of various types of normality tests. *Journal of Statistical Computation and Simulation*, 81(12), 2141–2155. <https://doi.org/10.1080/00949655.2010.520163>
- Yuzugullu, O., Erten, E., & Hajnsek, I. (2017). Estimation of Rice Crop Height from X-and C-Band PolSAR by Metamodel-Based Optimisation. *IEEE Journal of Selected Topics in Applied Earth Observations and Remote Sensing*, 10(1), 194–204. <https://doi.org/10.1109/JSTARS.2016.2575362>

7. APPENDICES

Appendix -I Ratoon and Non-ratoon crop samples

Province	Ratoon			Non-ratoon		
	FID_crop_no	HarMethod	Ecosystem	Non-ratoonFID	Ecosystem	HarMethod
Iloilo	F0621_1	mechanical	rainfed	F0625_1	rainfed	mechanical
Iloilo	F0629_1	manual	irrigated	F0630_1	irrigated	manual
Iloilo	F0640_1	mechanical	irrigated	F0639_0	irrigated	manual
Iloilo	F0643_0	mechanical	irrigated	F0638_0	irrigated	mechanical
Iloilo	F0643_1	mechanical	irrigated	F0638_1	irrigated	mechanical
Iloilo	F0643_2	mechanical	irrigated	F0637_2	irrigated	mechanical
Iloilo	F0649_1	manual	rainfed	F0647_1	rainfed	Manual
Iloilo	F0650_1	mechanical	rainfed	F0641_1	irrigated	mechanical
Iloilo	F0651_1	mechanical	irrigated	F0637_1	irrigated	mechanical
Iloilo	F0660_1	manual	rainfed	F0658_1	rainfed	Manual
Iloilo	F0666_1	manual	rainfed	F0672_0	rainfed	Manual
Iloilo	F0678_0	manual	rainfed	F0674_1	rainfed	Manual
Leyte	F0806_1	manual	irrigated	F0830_1	irrigated	manual
Leyte	F0806_2	manual	irrigated	F0849_2	irrigated	manual
Leyte	F0810_1	mechanical	irrigated	F0845_1	irrigated	mechanical
Leyte	F0810_2	mechanical	irrigated	F0826_2	irrigated	manual
Leyte	F0814_0	mechanical	rainfed	F0813_0	rainfed	mechanical
Leyte	F0827_1	manual	rainfed	F0815_1	rainfed	Manual
Leyte	F0830_2	manual	irrigated	F0825_2	irrigated	manual
Leyte	F0842_2	mechanical	rainfed	F0853_2	rainfed	mechanical
Leyte	F0846_1	manual	irrigated	F0829_1	irrigated	manual
Leyte	F0850_1	manual	rainfed	F0834_1	rainfed	Manual

DETECTING RATOON RICE AND MAPPING ITS DISTRIBUTION USING MACHINE LEARNING ALGORITHM AND SENTINEL-1 TIME SERIES DATA

Leyte	F0850_2	manual	rainfed	F0841_3	rainfed	Manual
Leyte	F0851_2	manual	rainfed	F0837_2	rainfed	Manual
Leyte	F0855_1	manual	irrigated	F0852_1	irrigated	manual
Leyte	F0857_0	manual	irrigated	F0852_0	irrigated	manual
Agusan del Sur	F1304_1	mechanical	irrigated	F1308_1	irrigated	mechanical
Agusan del Sur	F1304_2	mechanical	irrigated	F1305_1	irrigated	mechanical
Agusan del Sur	F1308_2	mechanical	irrigated	F1309_2	irrigated	mechanical
Agusan del Sur	F1312_2	mechanical	rainfed	F1346	rainfed	mechanical
Agusan del Sur	F1313_2	mechanical		F1320_2	irrigated	mechanical
Agusan del Sur	F1323_2	mechanical	irrigated	F1319_2	irrigated	mechanical
Agusan del Sur	F1345_1	manual	irrigated	F1339_1	irrigated	mechanical
Agusan del Sur	F1349_2	manual	irrigated	F1341_2	irrigated	mechanical
Agusan del Sur	F1359_2	manual	rainfed	F1352_2	rainfed	mechanical

Appendix -IIA: Confusion matrix, OOB estimated error rate and class error obtained from training dataset using random forest and VV, VH and VH/VV polarisations in the vegetative stage of ratoon and non-ratoon features.

Reference				
Features	Ratoon	Non-Ratoon	Total	Class Error
Ratoon	3	15	18	0.833
Non-Ratoon	11	13	24	0.458
Total	14	28	42	
OOB estimate of error rate: 61.90%				

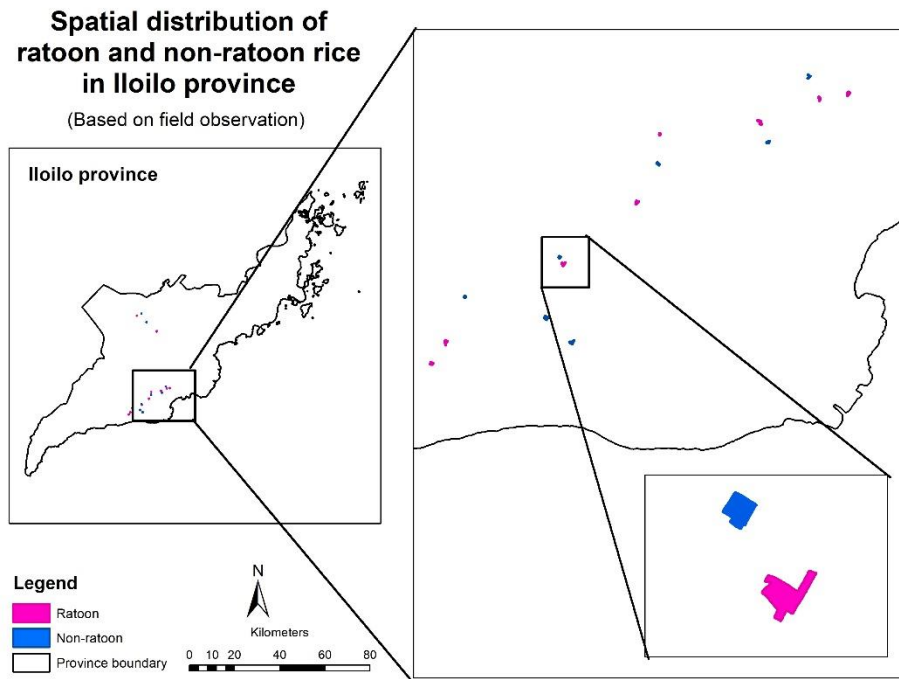
Appendix -IIB: Confusion matrix, OOB estimated error rate and class error obtained from training dataset using random forest and VV, VH and VH/VV polarisations in the flowering stage of ratoon and non-ratoon features.

Reference				
Features	Ratoon	Non-Ratoon	Total	Class Error
Ratoon	11	7	18	0.388
Non-Ratoon	5	19	24	0.208
Total	16	26	42	
OOB estimate of error rate 28.57%				

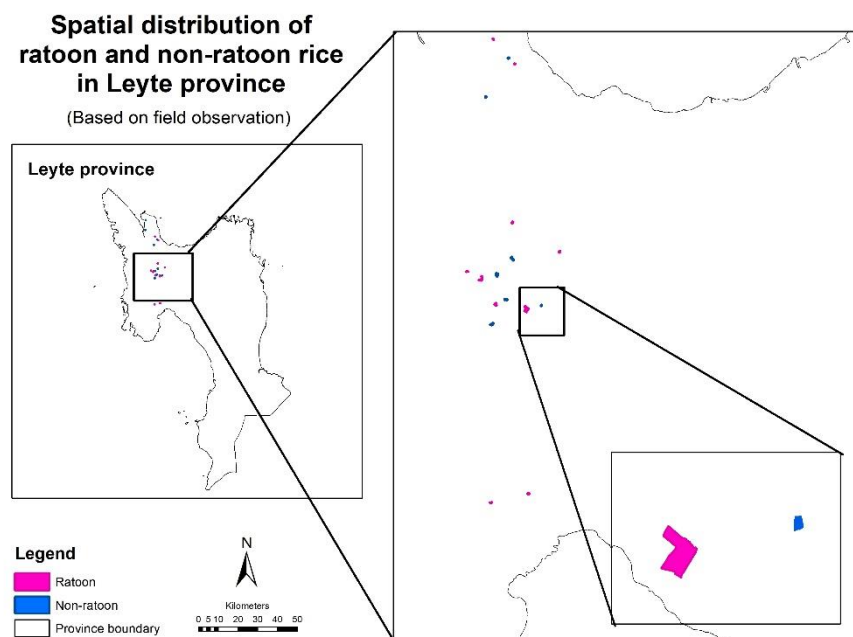
Appendix -IIC: Confusion matrix, OOB estimated error rate and class error obtained from training dataset using random forest and VV, VH and VH/VV polarisations in ripening stage of ratoon and non-ratoon features.

Reference				
Features	Ratoon	Non-Ratoon	Total	Class Error
Ratoon	14	4	18	0.222
Non-Ratoon	6	18	24	0.250
Total	20	22	42	
OOB estimate of error rate: 23.81%				

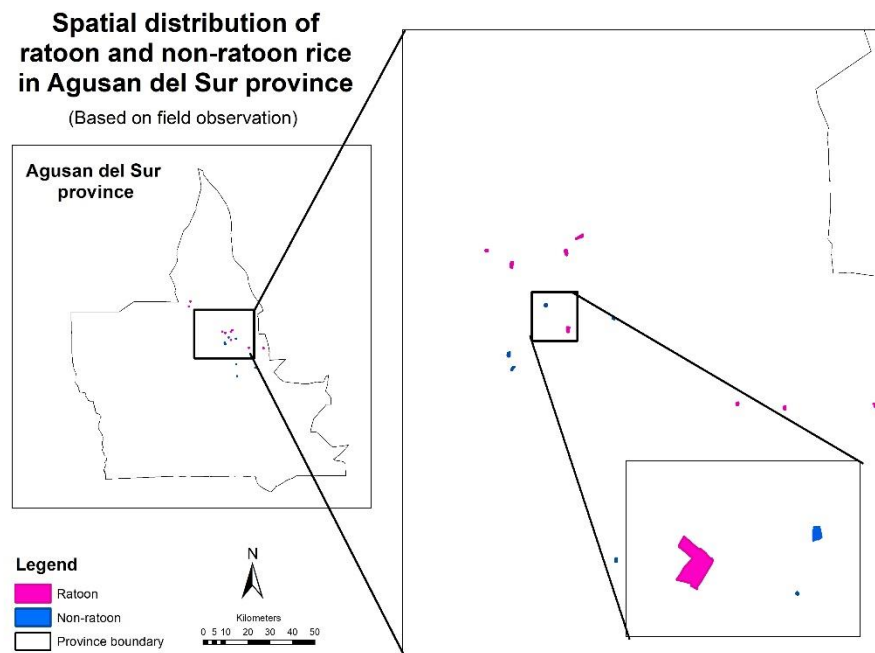
Appendix -IIIA: Map showing the spatial distribution of field observation of ratoon and non- ratoon rice during the study period (2017-2019) in the Leyte province



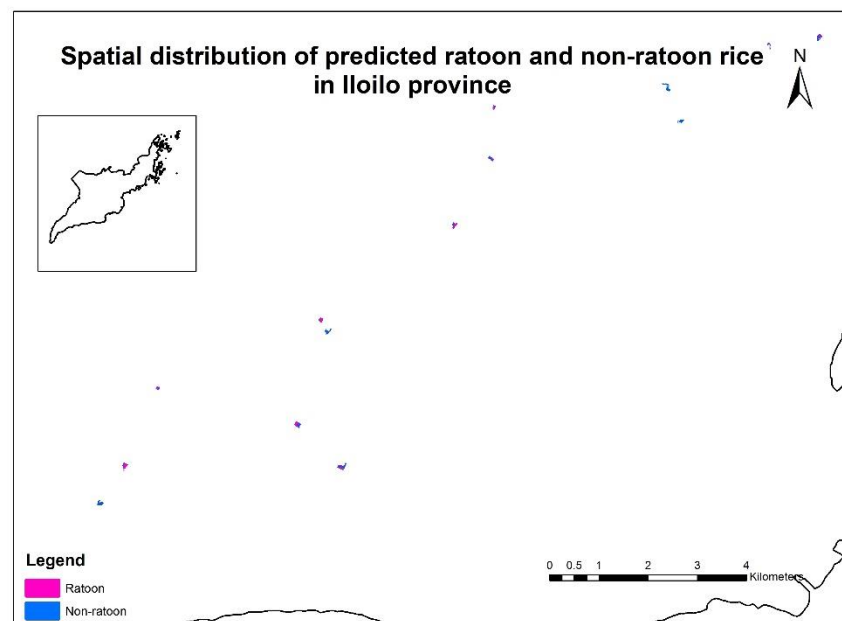
Appendix -IIIB: Map showing the spatial distribution of field observation of ratoon and non- ratoon rice during the study period (2017-2019) in the Iloilo province



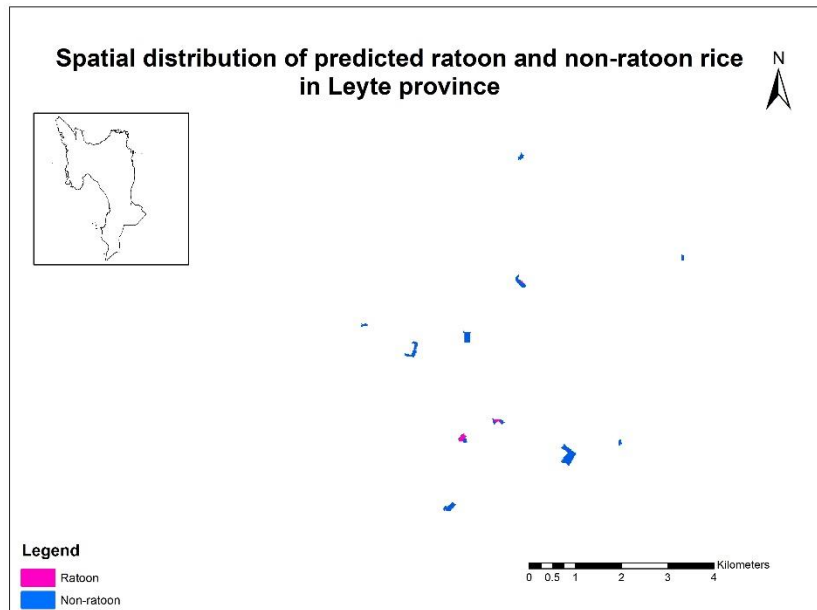
Appendix -IIIA: Map showing the spatial distribution of field observation of ratoon and non- ratoon rice during the study period (2017-2019) in the Agusan del Sur province



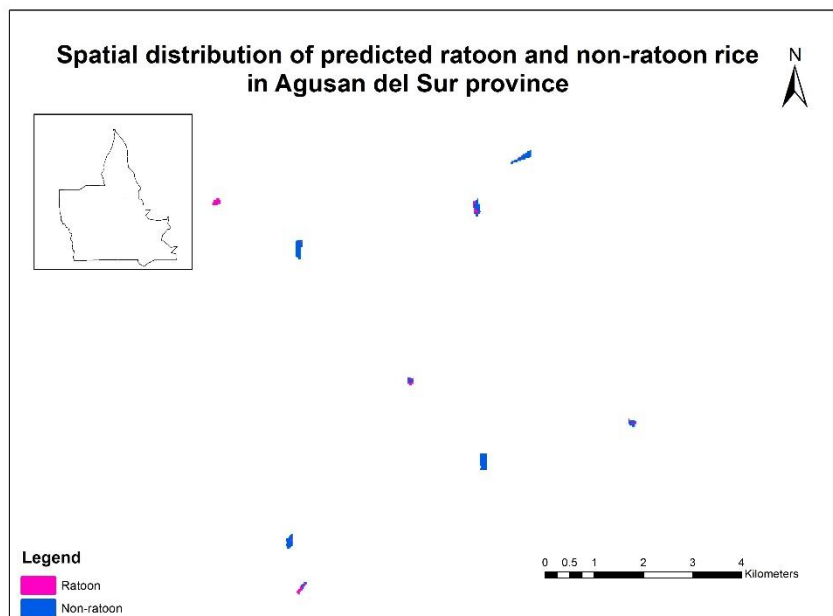
Appendix -IVA: Map showing the distribution of predicted ratoon and non- ratoon rice during the study period (2017-2019) in the Iloilo province



Appendix -IVB: Map showing the distribution of predicted ratoon and non- ratoon rice during the study period (2017-2019) in the Leyte province



Appendix -IVC: Map showing the distribution of predicted ratoon and non- ratoon rice during the study period (2017-2019) in the Agusan del Sur province



DETECTING RATOON RICE AND MAPPING ITS DISTRIBUTION USING MACHINE LEARNING ALGORITHM AND SENTINEL-1 TIME SERIES DATA

Appendix V: Data used for classification and Statistically test

Growth stages	VV	VH	VH-VV	category	class
Vegetative Phase	-9.33430944	-15.53960038	-6.20529094	1	Ratoon
Vegetative Phase	-9.51818124	-14.98518023	-5.46699899	1	Ratoon
Vegetative Phase	-11.98507598	-16.26103456	-4.27595858	1	Ratoon
Vegetative Phase	-9.04858447	-14.03927692	-4.99069245	1	Ratoon
Vegetative Phase	-9.61158373	-14.27127823	-4.65969450	1	Ratoon
Vegetative Phase	-10.72394366	-15.12962748	-4.40568382	1	Ratoon
Vegetative Phase	-9.28112045	-13.84313140	-4.56201095	1	Ratoon
Vegetative Phase	-8.50858337	-14.83000196	-6.32141859	1	Ratoon
Vegetative Phase	-11.27489863	-14.92656294	-3.65166431	1	Ratoon
Vegetative Phase	-8.36022489	-14.50534334	-6.14511845	1	Ratoon
Vegetative Phase	-10.15073114	-14.27302238	-4.12229124	1	Ratoon
Vegetative Phase	-8.35665694	-14.18323271	-5.82657577	1	Ratoon
Vegetative Phase	-8.04888600	-13.41154609	-5.36266009	1	Ratoon
Vegetative Phase	-7.96865761	-13.95938396	-5.99072635	1	Ratoon
Vegetative Phase	-8.67393063	-14.67630661	-6.00237598	1	Ratoon
Vegetative Phase	-8.60652464	-14.01022864	-5.40370400	1	Ratoon
Vegetative Phase	-11.75063851	-16.45113925	-4.70050074	1	Ratoon
Vegetative Phase	-7.22928254	-14.35512865	-7.12584611	1	Ratoon
Vegetative Phase	-8.32880394	-14.04382810	-5.71502416	1	Ratoon
Vegetative Phase	-7.69660358	-13.59380543	-5.89720185	1	Ratoon
Vegetative Phase	-8.64897018	-14.67690006	-6.02792988	1	Ratoon
Vegetative Phase	-10.15176784	-13.34835307	-3.19658523	1	Ratoon
Vegetative Phase	-9.12773774	-14.38769581	-5.25995807	1	Ratoon
Vegetative Phase	-9.30721408	-13.98296836	-4.67575428	1	Ratoon
Vegetative Phase	-8.28113626	-13.05419807	-4.77306181	1	Ratoon
Vegetative Phase	-9.79316164	-14.04662846	-4.25346682	1	Ratoon
Vegetative Phase	-7.05280306	-13.61195831	-6.55915525	1	Ratoon
Vegetative Phase	-9.36532872	-13.22476389	-3.85943517	1	Ratoon
Vegetative Phase	-8.58055806	-15.32264659	-6.74208854	1	Ratoon
Vegetative Phase	-8.71436165	-15.70151834	-6.98715669	1	Ratoon
Ripening Phase	-10.48063142	-14.99742601	-4.51679459	1	Ratoon
Ripening Phase	-10.61827169	-15.65267668	-5.03440499	1	Ratoon
Ripening Phase	-9.94755634	-16.49194384	-6.54438750	1	Ratoon
Ripening Phase	-9.75556852	-15.51666287	-5.76109435	1	Ratoon
Ripening Phase	-10.07237570	-13.28327390	-3.21089820	1	Ratoon
Ripening Phase	-9.36850991	-13.77091095	-4.40240104	1	Ratoon
Ripening Phase	-9.88194101	-15.43002281	-5.54808180	1	Ratoon
Ripening Phase	-8.94327912	-13.62595841	-4.68267929	1	Ratoon
Ripening Phase	-10.89236405	-15.64933632	-4.75697227	1	Ratoon
Ripening Phase	-9.28180644	-15.52179063	-6.23998419	1	Ratoon
Ripening Phase	-9.79930544	-15.42883104	-5.62952560	1	Ratoon

DETECTING RATOON RICE AND MAPPING ITS DISTRIBUTION USING MACHINE LEARNING ALGORITHM AND SENTINEL-1 TIME SERIES DATA

Ripening Phase	-8.03776996	-13.23709818	-5.19932822	1	Ratoon
Ripening Phase	-8.62605272	-13.93690311	-5.31085039	1	Ratoon
Ripening Phase	-8.00505093	-13.79484197	-5.78979104	1	Ratoon
Ripening Phase	-10.27066400	-15.39643292	-5.12576892	1	Ratoon
Ripening Phase	-9.16650957	-14.62237052	-5.45586095	1	Ratoon
Ripening Phase	-8.59456114	-14.58622623	-5.99166509	1	Ratoon
Ripening Phase	-6.58419295	-13.29299570	-6.70880275	1	Ratoon
Ripening Phase	-8.01749955	-13.80221430	-5.78471475	1	Ratoon
Ripening Phase	-8.59935073	-14.31020889	-5.71085816	1	Ratoon
Ripening Phase	-12.74321658	-18.82275145	-6.07953487	1	Ratoon
Ripening Phase	-8.63648720	-14.15058503	-5.51409783	1	Ratoon
Ripening Phase	-10.74272424	-15.06685809	-4.32413385	1	Ratoon
Ripening Phase	-9.10166678	-14.22723962	-5.12557284	1	Ratoon
Ripening Phase	-10.02483801	-15.42842854	-5.40359053	1	Ratoon
Ripening Phase	-8.94928310	-13.29422286	-4.34493976	1	Ratoon
Ripening Phase	-7.19574494	-13.66747211	-6.47172717	1	Ratoon
Ripening Phase	-11.09997811	-16.12986547	-5.02988735	1	Ratoon
Ripening Phase	-8.62605272	-14.00228848	-5.37623576	1	Ratoon
Ripening Phase	-8.03339177	-13.64804178	-5.61465002	1	Ratoon
Flowering Phase	-10.29806023	-15.52081621	-5.22275598	1	Ratoon
Flowering Phase	-9.11233901	-15.17510773	-6.06276872	1	Ratoon
Flowering Phase	-10.81310786	-15.83504408	-5.02193622	1	Ratoon
Flowering Phase	-9.53414304	-14.04515300	-4.51100996	1	Ratoon
Flowering Phase	-11.21429525	-15.95054321	-4.73624796	1	Ratoon
Flowering Phase	-10.63810177	-15.35525526	-4.71715349	1	Ratoon
Flowering Phase	-10.13984723	-15.06406875	-4.92422152	1	Ratoon
Flowering Phase	-8.90652858	-14.39773453	-5.49120595	1	Ratoon
Flowering Phase	-10.58470019	-15.50014227	-4.91544208	1	Ratoon
Flowering Phase	-9.08175357	-14.36092000	-5.27916643	1	Ratoon
Flowering Phase	-10.61735709	-15.57484805	-4.95749096	1	Ratoon
Flowering Phase	-8.54456494	-14.47315085	-5.92858591	1	Ratoon
Flowering Phase	-8.63001035	-14.27657172	-5.64656137	1	Ratoon
Flowering Phase	-8.24089847	-13.27574854	-5.03485007	1	Ratoon
Flowering Phase	-9.64035128	-15.03939826	-5.39904698	1	Ratoon
Flowering Phase	-8.01480751	-14.29630719	-6.28149968	1	Ratoon
Flowering Phase	-10.20436229	-14.84946324	-4.64510095	1	Ratoon
Flowering Phase	-7.22928254	-13.40842273	-6.17914019	1	Ratoon
Flowering Phase	-7.36371103	-13.52938671	-6.16567568	1	Ratoon
Flowering Phase	-8.36739717	-14.25803764	-5.89064047	1	Ratoon
Flowering Phase	-12.13918438	-18.53387550	-6.39469112	1	Ratoon
Flowering Phase	-8.17079675	-13.41917284	-5.24837609	1	Ratoon
Flowering Phase	-9.45738798	-13.98869970	-4.53131172	1	Ratoon
Flowering Phase	-9.40177395	-13.49748281	-4.09570886	1	Ratoon
Flowering Phase	-8.62048074	-13.71611902	-5.09563828	1	Ratoon

DETECTING RATOON RICE AND MAPPING ITS DISTRIBUTION USING MACHINE LEARNING ALGORITHM AND SENTINEL-1 TIME SERIES DATA

Flowering Phase	-8.54441697	-12.80204896	-4.25763199	1	Ratoon
Flowering Phase	-7.05280306	-13.61195831	-6.55915525	1	Ratoon
Flowering Phase	-9.47011137	-14.33937835	-4.86926698	1	Ratoon
Flowering Phase	-8.63001035	-14.22680751	-5.59679716	1	Ratoon
Flowering Phase	-7.87733880	-12.57878227	-4.70144347	1	Ratoon
Vegetative Phase	-9.76705735	-17.02243125	-7.25537390	2	Non-Ratoon
Vegetative Phase	-10.47724426	-14.53105392	-4.05380966	2	Non-Ratoon
Vegetative Phase	-9.90690836	-14.95359808	-5.04668972	2	Non-Ratoon
Vegetative Phase	-8.53193463	-15.23914349	-6.70720886	2	Non-Ratoon
Vegetative Phase	-8.47073055	-14.93206243	-6.46133188	2	Non-Ratoon
Vegetative Phase	-11.08995251	-16.01022318	-4.92027067	2	Non-Ratoon
Vegetative Phase	-9.84551456	-15.11521201	-5.26969746	2	Non-Ratoon
Vegetative Phase	-11.47219917	-15.44491086	-3.97271169	2	Non-Ratoon
Vegetative Phase	-10.34066705	-15.73676854	-5.39610149	2	Non-Ratoon
Vegetative Phase	-10.55801801	-14.87373233	-4.31571432	2	Non-Ratoon
Vegetative Phase	-8.37294251	-14.50276028	-6.12981777	2	Non-Ratoon
Vegetative Phase	-8.34466754	-13.91610648	-5.57143894	2	Non-Ratoon
Vegetative Phase	-8.64811609	-14.12661352	-5.47849743	2	Non-Ratoon
Vegetative Phase	-10.94846202	-14.87876734	-3.93030532	2	Non-Ratoon
Vegetative Phase	-7.43856702	-14.20417430	-6.76560729	2	Non-Ratoon
Vegetative Phase	-8.92099250	-14.78934791	-5.86835541	2	Non-Ratoon
Vegetative Phase	-8.02174250	-14.29861328	-6.27687078	2	Non-Ratoon
Vegetative Phase	-8.99927348	-14.18963426	-5.19036078	2	Non-Ratoon
Vegetative Phase	-8.75997556	-14.52730592	-5.76733036	2	Non-Ratoon
Vegetative Phase	-10.25786197	-14.96177469	-4.70391272	2	Non-Ratoon
Vegetative Phase	-8.32725728	-13.46083195	-5.13357467	2	Non-Ratoon
Vegetative Phase	-8.92355925	-13.31356947	-4.39001022	2	Non-Ratoon
Vegetative Phase	-10.27692026	-16.25853213	-5.98161187	2	Non-Ratoon
Vegetative Phase	-8.79232272	-12.96004948	-4.16772676	2	Non-Ratoon
Vegetative Phase	-9.55406724	-14.47352336	-4.91945612	2	Non-Ratoon
Vegetative Phase	-9.20709137	-14.68040992	-5.47331855	2	Non-Ratoon
Vegetative Phase	-11.04170449	-15.68102021	-4.63931572	2	Non-Ratoon
Vegetative Phase	-9.69208528	-15.15637233	-5.46428705	2	Non-Ratoon
Vegetative Phase	-8.56595626	-14.86146172	-6.29550546	2	Non-Ratoon
Vegetative Phase	-9.46133094	-14.06179213	-4.60046119	2	Non-Ratoon
Ripening Phase	-9.56537382	-16.44777680	-6.88240298	2	Non-Ratoon
Ripening Phase	-9.54163997	-18.13585801	-8.59421805	2	Non-Ratoon
Ripening Phase	-12.15308420	-19.78266184	-7.62957764	2	Non-Ratoon
Ripening Phase	-10.47669431	-14.92028106	-4.44358675	2	Non-Ratoon
Ripening Phase	-9.75940848	-17.19968716	-7.44027868	2	Non-Ratoon
Ripening Phase	-11.02516383	-16.98360939	-5.95844556	2	Non-Ratoon
Ripening Phase	-7.89400565	-16.57543924	-8.68143359	2	Non-Ratoon
Ripening Phase	-10.41534374	-15.21491098	-4.79956724	2	Non-Ratoon
Ripening Phase	-9.60464379	-16.15570317	-6.55105938	2	Non-Ratoon

DETECTING RATOON RICE AND MAPPING ITS DISTRIBUTION USING MACHINE LEARNING ALGORITHM AND SENTINEL-1 TIME SERIES DATA

Ripening Phase	-10.30155723	-17.40002021	-7.09846298	2	Non-Ratoon
Ripening Phase	-10.28192306	-16.78768213	-6.50575907	2	Non-Ratoon
Ripening Phase	-12.12839302	-18.34428625	-6.21589323	2	Non-Ratoon
Ripening Phase	-8.37756321	-12.67623529	-4.29867208	2	Non-Ratoon
Ripening Phase	-13.91192922	-20.55375733	-6.64182811	2	Non-Ratoon
Ripening Phase	-9.22685221	-15.54765133	-6.32079912	2	Non-Ratoon
Ripening Phase	-8.40862069	-14.18656331	-5.77794262	2	Non-Ratoon
Ripening Phase	-10.76597729	-17.47975175	-6.71377446	2	Non-Ratoon
Ripening Phase	-10.03506981	-17.27399556	-7.23892575	2	Non-Ratoon
Ripening Phase	-10.04012357	-16.00090011	-5.96077654	2	Non-Ratoon
Ripening Phase	-9.36834601	-14.51792140	-5.14957540	2	Non-Ratoon
Ripening Phase	-9.70441584	-20.45269265	-10.74827681	2	Non-Ratoon
Ripening Phase	-11.31859593	-20.48302749	-9.16443156	2	Non-Ratoon
Ripening Phase	-9.98135118	-16.52412931	-6.54277813	2	Non-Ratoon
Ripening Phase	-8.57919836	-18.77279256	-10.19359420	2	Non-Ratoon
Ripening Phase	-10.99047682	-18.30054833	-7.31007151	2	Non-Ratoon
Ripening Phase	-8.61051432	-14.18111540	-5.57060108	2	Non-Ratoon
Ripening Phase	-9.70292974	-16.36772945	-6.66479971	2	Non-Ratoon
Ripening Phase	-13.36666756	-15.22576541	-1.85909785	2	Non-Ratoon
Ripening Phase	-11.86921435	-13.52437128	-1.65515693	2	Non-Ratoon
Ripening Phase	-8.61051432	-20.42051912	-11.81000480	2	Non-Ratoon
Flowering Phase	-8.28146411	-16.37771623	-8.09625212	2	Non-Ratoon
Flowering Phase	-9.44707308	-17.39697333	-7.94990025	2	Non-Ratoon
Flowering Phase	-11.00562919	-17.55272774	-6.54709855	2	Non-Ratoon
Flowering Phase	-9.18017089	-16.28390474	-7.10373386	2	Non-Ratoon
Flowering Phase	-10.75176549	-15.50660852	-4.75484303	2	Non-Ratoon
Flowering Phase	-11.12599457	-16.45654651	-5.33055194	2	Non-Ratoon
Flowering Phase	-11.45806832	-17.65041219	-6.19234387	2	Non-Ratoon
Flowering Phase	-11.15816265	-15.20403799	-4.04587534	2	Non-Ratoon
Flowering Phase	-10.26581921	-16.33370308	-6.06788387	2	Non-Ratoon
Flowering Phase	-11.01874722	-16.58735880	-5.56861158	2	Non-Ratoon
Flowering Phase	-9.78911328	-14.92853543	-5.13942215	2	Non-Ratoon
Flowering Phase	-8.93370368	-13.78760126	-4.85389758	2	Non-Ratoon
Flowering Phase	-9.09992170	-14.20261968	-5.10269798	2	Non-Ratoon
Flowering Phase	-8.50831619	-14.41440085	-5.90608466	2	Non-Ratoon
Flowering Phase	-8.26585996	-14.38868718	-6.12282722	2	Non-Ratoon
Flowering Phase	-9.15847353	-14.16712090	-5.00864737	2	Non-Ratoon
Flowering Phase	-9.21684842	-13.04346891	-3.82662049	2	Non-Ratoon
Flowering Phase	-8.45808906	-13.26884966	-4.81076060	2	Non-Ratoon
Flowering Phase	-9.16941002	-14.83933021	-5.66992020	2	Non-Ratoon
Flowering Phase	-9.59499831	-15.38950139	-5.79450308	2	Non-Ratoon
Flowering Phase	-8.51708624	-14.77180003	-6.25471379	2	Non-Ratoon
Flowering Phase	-8.18224104	-18.77400333	-10.59176229	2	Non-Ratoon
Flowering Phase	-9.44043644	-14.19985700	-4.75942056	2	Non-Ratoon

DETECTING RATOON RICE AND MAPPING ITS DISTRIBUTION USING MACHINE LEARNING ALGORITHM AND
SENTINEL-1 TIME SERIES DATA

Flowering Phase	-10.94005944	-16.62055654	-5.68049710	2	Non-Ratoon
Flowering Phase	-8.86885211	-14.61336978	-5.74451767	2	Non-Ratoon
Flowering Phase	-9.34553754	-14.85965476	-5.51411723	2	Non-Ratoon
Flowering Phase	-8.40298452	-13.92815296	-5.52516844	2	Non-Ratoon
Flowering Phase	-12.95120917	-13.13628948	-0.18508031	2	Non-Ratoon
Flowering Phase	-8.41820826	-14.23571898	-5.81751072	2	Non-Ratoon
Flowering Phase	-8.20946283	-18.22630340	-10.01684057	2	Non-Ratoon

Appendix VI: Code used for classification at different growth stages

###Sentinel-1 backscatter data classification

only install libraries if needed, i.e. - only do this once

if (!require("raster")) install.packages("raster")

if (!require("sf")) install.packages("sf")

if (!require("rgdal")) install.packages("rgdal")

if (!require("randomForest")) install.packages("random Forest")

if (!require("caret")) install. Packages("caret")

add packages

library("spy")

library("raster")

library("map tools")

library("rgdal")

library("disco")

stewed("C:/RF/new_dataset")

Read Data - I added a line here for my computer, you need to comment it out and replace with your path_to_file

data <- read.csv("class_file_latest.csv", header = TRUE)

#data <- read.csv("VH_R", header = TRUE)

d<-within(data, rm("class"))

d

str(d)

change the category column to a factor

d\$category <- as.factor(d\$category)

table(d\$category)

Partition the data into train and test sets

set.seed(123)

ind <- sample(2, nrow(d), replace = TRUE, prob = c(0.7, 0.3))

train <- d[ind==1,]

test <- d[ind==2,]

grid search approach to tune the RF model using caret () library functionality

we will do a 10 fold cross validation, repeated three times

control <- trainControl(

 method="repeatedcv",

 number=10,

 repeats=3,

 search="grid"

```
)

#set the accuracy metric for random forest classification
metric <- "Accuracy"
# tune the rf with a grid search (actually a vector search since we only search for best mtry)
tuneGrid <- expand.grid(mtry=c(1:15))
rf_gridsearch <- train(category~.,
  data = train,
  method = "rf",
  metric = metric,
  tuneGrid = tuneGrid,
  trControl = control
)
print(rf_gridsearch)
plot(rf_gridsearch)
# train the random forest model on the best mtry
rf_out <- randomForest(category~.,
  data = train,
  mtry = rf_gridsearch$bestTune$mtry,
  ntree = 300
)
# view the confusion matrix for the trained model
rf_out
# plot the size of trees in an ensemble
hist(treesize(rf_out),
  main = "No. of Nodes for the Trees",
  col = "green")
#view the variable importance of the trained model
importance(rf_out)
# plot the variable importance of the trained model
varImpPlot(rf_out,
  sort = T,
  n.var = 3,
  main = "Variable Importance")
# Use the trained model on the test dataset
p_out <- predict(
  object = rf_out,
  newdata = test
)
# view the predicted values
p_out
# print the confusion matrix
confusionMatrix(p_out, test$category)
### To predict with Sentinel-1 image data
files <- list.files(path = "C:/RF/new_dataset", pattern = ".tif", full.names=TRUE)
files
```

```
#predictors <- brick( "C:/RF/new_dataset/Sigma0_VV_db_CompositeBands1.tif.tif")
predictors1 <- brick( "C:/RF/new_dataset/layerstcekd.tif.tif")
predictors1
names(predictors1)<-c('VV', 'VH', 'VH.VV')
predictors1
classifiedS1P<-predict(predictors1, rf_out, type='response', progress='window')
classifiedS1P
par(mfrow=c(1,2))
plot(classifiedS1P)
writeRaster(classifiedS1P, "C:/RF/", format="GTiff", datatype='INT1U', overwrite=TRUE)
#write out the predicted classification to a raster file
```

Appendix VII: Matlab code for plotting line graph for ratoon and non-ratoon rice field in Iloilo province in wet season 2018 through VV,VH and VH/VV polarisations

```
% ratoon and non-ratoon for VH
IIS2_650= IlloiloVH(:,21:40)
Iiwetseason2018=IlloiloDates(21:40)'
t = datetime(Iiwetseason2018,'InputFormat','dd-MM-yyyy')
hold on
%ratoon and non-ratoon for VH : plotting
ratoonIIS2_650 = IIS2_650([15],:)
non_ratoonS2_I1661=IIS2_650([ 25],:);
plot(t(1:20),ratoonIIS2_650(1:end),"LineStyle","--","Marker","d","Color","m")
plot(t(1:20),non_ratoonS2_I1661(1:end),"LineStyle","--","Marker","d","Color","k')
% creating vertical lines
Rat_1= datetime(2018,11,18).
line([Rat_1 Rat_1],ylim,'Color','r','LineStyle','-').
str_text_harv={' RHD 18/11/2018', ''}
harves=text([Rat_1 Rat_1], ylim,str_text_harv);
set(harves,'Rotation',90)
NonRat_1= datetime(2018,10,04);
line([NonRat_1 NonRat_1],ylim,'Color','k','LineStyle','-');
str_harv_NonRat_1={' HD 04/10/2018', ''};
harvest_date_1=text([NonRat_1 NonRat_1], ylim,str_harv_NonRat_1);
set(harvest_date_1,'Rotation',90)
% Giving legend for VH in ratoon and non-ratoon
xlabel('Dates')
ylabel('Backscatter response')
legend('Ratoon riceVH F0650','Non-ratoon riceVH F0661')
title(' Ratoon and non ratoon rice backscatter responses: Iloilo wet season 2018 ')
hold off
% VV
IIS2_650VV= IlloiloVV(:,21:40)
Iiwetseason2018VV=IlloiloDates(21:40)'
ttimevv = datetime(Iiwetseason2018VV,'InputFormat','dd-MM-yyyy')
hold on
%Plotting of ratoon and non-ratoon in VV
ratoonIIS2_650VV = IIS2_650VV([15],:)
```

```

non_ratoonS2_II661VV=IIS2_650VV([ 25],:);
plot(t(1:20),ratoonIIS2_650VV(1:end),"LineStyle","-","Marker","d","Color","m")
plot(t(1:20),non_ratoonS2_II661VV(1:end),"LineStyle","-","Marker","d","Color","k')
% Creating vertival lines
Rat_1= datetime(2018,11,18);
line([Rat_1 Rat_1],ylim,'Color','r','LineStyle','-');
strr_text_harv={' RHD 18/11/2018', ''}
harves=text([Rat_1 Rat_1], ylim,strr_text_harv);
set(harves,'Rotation',90)
NonRat_1= datetime(2018,10,04);
line([NonRat_1 NonRat_1],ylim,'Color','k','LineStyle','-');
str_harv_NonRat_1={' HD 04/10/2018', ''};
harvest_date_1=text([NonRat_1 NonRat_1], ylim,str_harv_NonRat_1);
set(harvest_date_1,'Rotation',90)
% Legend in VV
xlabel('Dates')
ylabel('Backscatter response')
legend('Ratoon rice VV F0650','Non-ratoon rice VV F0661')
title(' Ratoon and non ratoon rice backscatter responses in VV: Iloilo wet season 2018 ')
hold off
% ratoon and non-ratoon VH/VV ratio
ratioVHV650Ratoon=minus(ratoonIIS2_650,ratoonIIS2_650VV)
ratioVHV661NonRatoon=minus(non_ratoonS2_II661,non_ratoonS2_II661VV)
Iiwetseason2018VV=IloiloDates(21:40)'
ttimevv = datetime(Iiwetseason2018VV,'InputFormat','dd-MM-yyyy')
hold on
plot(t(1:20),ratioVHV650Ratoon(1:end),"LineStyle","-","Marker","d","Color","m')
plot(t(1:20),ratioVHV661NonRatoon(1:end),"LineStyle","-","Marker","d","Color","k')
% creating vertical lines
Rat_1= datetime(2018,11,18);
line([Rat_1 Rat_1],ylim,'Color','r','LineStyle','-');
strr_text_harv={' RHD 18/11/2018', ''}
harves=text([Rat_1 Rat_1], ylim,strr_text_harv);
set(harves,'Rotation',90)
NonRat_1= datetime(2018,10,04);
line([NonRat_1 NonRat_1],ylim,'Color','k','LineStyle','-');
str_harv_NonRat_1={' HD 04/10/2018', ''};
harvest_date_1=text([NonRat_1 NonRat_1], ylim,str_harv_NonRat_1);
set(harvest_date_1,'Rotation',90)
% Legend of VH/VV in raoon and non-ratoon
xlabel('Dates')
ylabel('Backscatter response')
legend('Ratoon rice VHV F0650','Non-ratoon rice VHV F0661')
title(' Ratoon and non ratoon rice backscatter responses in VH/VV: Iloilo wet season 2018 ')
hold off

```

Appendix VIII: The Google Earth Engine code used for downloading Sentinel-1 images

```

// Load Sentinel-1 C-band SAR Ground Range collection (log scale, VV, descending)
var collectionVV = ee.ImageCollection('COPERNICUS/S1_GRD')
.filter(ee.Filter.eq('instrumentMode', 'TW'))

```

```
.filter(ee.Filter.listContains('transmitterReceiverPolarisation', 'VV'))
.filter(ee.Filter.eq('orbitProperties_pass', 'DESCENDING'))
.filterMetadata('resolution_meters', 'equals', 10)
.filterBounds(table3)
.select('VV');
print(collectionVV, 'Collection VV');
// Load Sentinel-1 C-band SAR Ground Range collection (log scale, VH, descending)
var collectionVH = ee.ImageCollection('COPERNICUS/S1_GRD')
.filter(ee.Filter.eq('instrumentMode', 'TW'))
.filter(ee.Filter.listContains('transmitterReceiverPolarisation', 'VH'))
.filter(ee.Filter.eq('orbitProperties_pass', 'DESCENDING'))
.filterMetadata('resolution_meters', 'equals', 10)
.filterBounds(table3)
.select('VH');
print(collectionVH, 'Collection VH');
//Filter by date
var VV2 = collectionVV.filterDate('2018-12-16', '2018-12-28').mosaic();
var VH2 = collectionVH.filterDate('2018-12-16', '2018-12-28').mosaic();
print(VV2, 'VV2');
print(VH2, 'VH2');
//Filter by date
var VV2 = collectionVV.filterDate('2018-12-16', '2018-12-28').mosaic();
var VH2 = collectionVH.filterDate('2018-12-16', '2018-12-28').mosaic();
// Display map
Map.centerObject(table3, 7);
Map.addLayer(VV2, {min:-15,max:0}, 'VV2', 0);
Map.addLayer(VH2, {min:-15,max:0}, 'VH2', 0);
//Apply filter to reduce speckle
var SMOOTHING_RADIUS = 50;
var VV2_filtered = VV2.focal_mean(SMOOTHING_RADIUS, 'circle', 'meters');
var VH2_filtered = VH2.focal_mean(SMOOTHING_RADIUS, 'circle', 'meters');
//Display filtered images
Map.addLayer(VV2_filtered.clip(table3), {min:-15,max:0}, 'VV2_Filtered',0);
Map.addLayer(VH2_filtered.clip(table3), {min:-15,max:0}, 'VH2_Filtered',0);
Export.image.toDrive({
  image: VH2_filtered,
  description: 'VH2_filtered',
  scale: 20,
  crs: 'EPSG:4326',
  maxPixels: 1e9,
  region: table3
});

Export.image.toDrive({
  image: VV2_filtered,
  description: 'VV2_filtered',
```


DETECTING RATOON RICE AND MAPPING ITS DISTRIBUTION USING MACHINE LEARNING ALGORITHM AND SENTINEL-1 TIME SERIES DATA

```
scale: 20,  
crs: 'EPSG:4326',  
maxPixels: 1e9,  
region: table3  
});
```

